Review Article

Bridged Benzocyclotrimers: concepts, Synthesis, and Applications

Sergio Cossu[a], Paola Peluso[b,*]

[a]Dipartimento di Scienze Molecolari e Nanosistemi DSMN, Università Ca' Foscari Venezia, Via Torino 155, I-30172 Mestre Venezia, Italy
[b]Istituto di Chimica Biomolecolare ICB, CNR, Sede secondaria di Sassari, Traversa La Crucca 3, Li Punti, I-07100 Sassari, Italy

* Corresponding author. E-mail address: paola.peluso@cnr.it. Tel.: +39 079 2841218.

ABSTRACT Bridged polycyclic frameworks represent a unique tool to form curved units, the bicyclo[2.2.1]hepta-2,5-diene system, being widely exploited to design and induce concave topologies. In particular, bridged benzocyclotrimers (BCTs) are characterized by a flat aromatic base decorated with bridged polycyclic motifs, which provide the suitable curvature underlying the concave-convex topology. In the 1960s, these molecules attracted interest for their own chemical and physical properties. Later, the improvements of synthetic procedures to produce bridged BCTs have paved the way for their utilization to design and prepare molecular containers, bowls, cages, and baskets that are able to accommodate target molecules, recognize them, and modulate their functions. In this frame, we aim to describe the historical evolution of the concept, from the first bridged BCTs explored to confirm the existence of strained alkynes, and the phenomenon of bond alternation (Mills-Nixon hypothesis), to the most recent gated molecular baskets developed as dynamic synthetic receptors for molecular delivery. The main synthetic approaches which have been used to perform cyclotrimerization of bridged polycyclic alkenes, and related mechanisms, are also examined and discussed, with a specific focus on the *syn*/*anti* stereoselectivity issue and its consequences at a mechanistic level.

Keywords: Benzocyclotrimers, cyclotrimerization, Mills-Nixon, molecular baskets, molecular recognition, polycyclic alkenes.

1. INTRODUCTION

In the last few decades, the chemistry of molecular hosts such as containers, bowls, cages, baskets, tweezers has attracted a growing interest on the basis of the concept that when a molecular species enters in the cavity of a synthetic receptor, its properties are different compared to those expressed in the bulk [1-3]. The properties of the internal surface of the concave receptor, shape and size of the confined space, and functional groups located at the rim of the gap are the factors which may impact the behavior of the guest and its motion, in a way mimicking natural molecular cavities such as those of enzymes and receptors. Concave surfaces are also of interest as complementary counterparts of the fullerene surface and other convex molecular units [4].

Starting from the late 20th century, bowl-shaped hydrocarbons with curved networks of trigonal carbon atoms have attracted interest as models and synthetic intermediates of more complex molecules characterized by curve surfaces such as C_{60} and the higher fullerenes [5-8]. Curved molecular surfaces featuring bowl-shaped π-conjugated motifs may be challenging to synthesize due to the presence of unusual angular strains [9]. The synthesis of corannulene (**1**), a subunit of fullerene (**2**) with C_{5v} symmetry (Fig. 1), was reported for the first time by Barth *et al*. in the late 1960s [10, 11] through a multistep process. However, it was later that the development of kilogram-scale synthesis allowed corannulene to become commercially available [12].

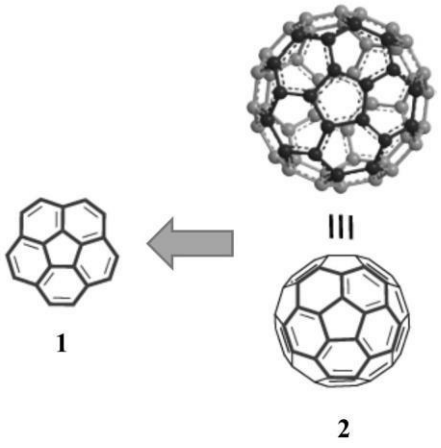

Fig. 1. Representation of corannulene (**1**) as a subunit of fullerene (C_{60}) (**2**) (adapted with permission from ref. 9).

Due to the distortion of the π-conjugation, in buckybowl structures an inefficient overlap of each p-orbital and an increase of the s-orbital character in sp^2 carbon occur compared to that of flat π-conjugation [6]. The distorted π-conjugation induces the curvature which identifies two faces, a concave face and a convex face, which may exhibit different stereoelectronic properties [6, 13]. If the bowl size is small enough to overcome the high-energy barrier of the transition state, bowl-shaped π-conjugated molecules exhibit the so-called bowl-to-bowl inversion, the interconversion of concave and convex faces (Fig. 2). This type of inversion has been studied in **1** [14-17] and sumanene (**3**) [18] at both experimental and computational level. It is worth mentioning that buckybowl molecules may possess inherent chirality which is often defined as "bowl chirality" [19].

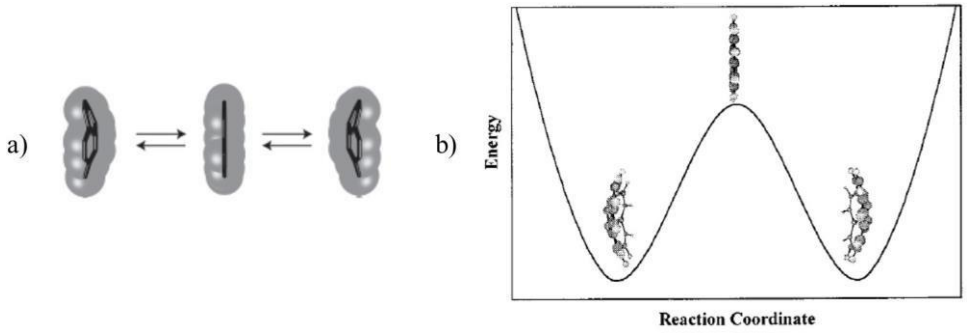

Fig. 2. a) Bowl-to-bowl inversion of **1** (adapted with permission from ref. 16); b) energy diagram of the inversion process of **1** (adapted with permission from ref. [14]).

Benzocyclotrimers (BCTs) are highly symmetric rigid molecules characterized by the presence of a central benzene ring fused to three bicycles, which have been widely used as important precursors to construct curved surfaces [9, 20, 21]. In 1996 Scott *et al*. obtained circumtrindene (**4**) by triple cyclodehydrogenation of decacyclene (**5**) through flash vacuum pyrolysis (FVP) (Scheme 1) [5, 22, 23].

While the simplest BCT triphenylene (**6**) is a planar molecule [24], **5** was shown to be twisted into a shallow molecular propeller due to nonbonded repulsion between hydrogens of the peripheral naphthalene groups [25]. More flexible BCTs were developed later, such as **7**-**11** containing three non-planar branches decorating the central aromatic ring (Fig. 3) [26-29].

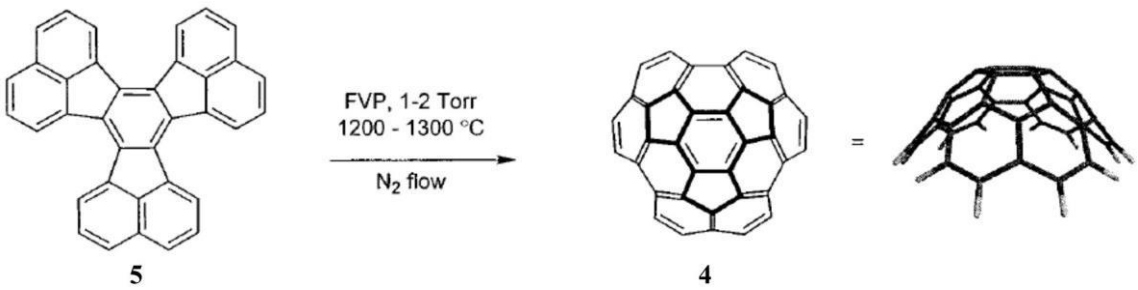

106106 **5** **4**

107 **Scheme 1.** Synthesis of circumtrindene (**4**) by triple dehydrogenation of decacyclene (**5**) (adapted with permission from

108 ref. 23).

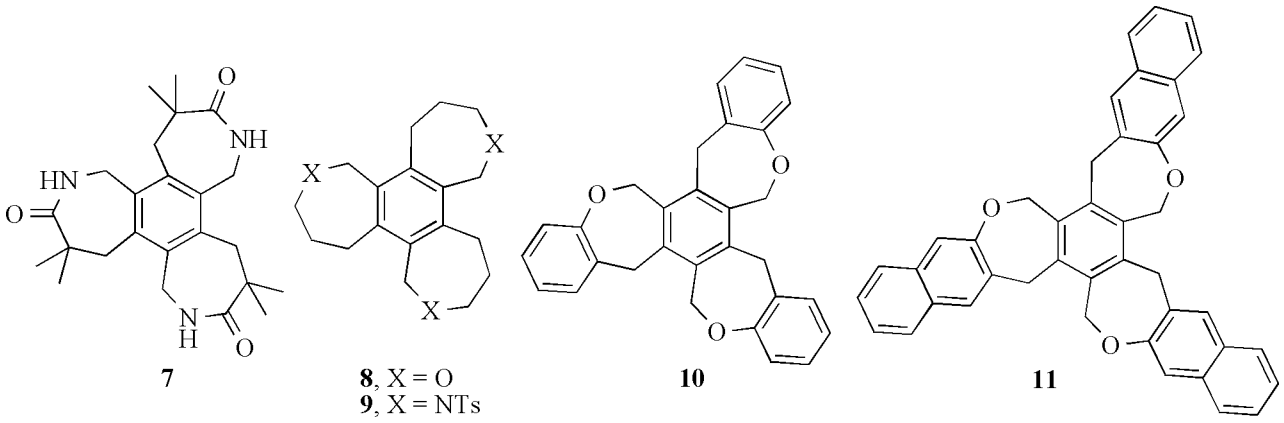

7 **8**, X = O; **9**, X = NTs **10** **11**

109

110 **Fig. 3.** Flexible benzocyclotrimers **7**–**11**.

111 Bridged polycyclic skeletons are characterized by a concave motif which is inherent to their strained

112 structure (Fig. 4). This feature has been fruitfully exploited to build concave molecules and curved

113 synthetic intermediates. Indeed, BCTs obtained by cyclotrimerization of bridged polycyclic alkenes are

114 characterized by a flat aromatic base decorated with bridged polycyclic units which provide the suitable

115 "natural" curvature underlying concave-convex topology. Depending on the relative topological

116 assembly of the three monomers in the cyclotrimerization process, in principle two diastereoisomers can

117 be obtained, the C_3 symmetric *syn*-isomer and the C_s symmetric *anti*-isomer (Fig. 5a) [20].

118 In 2003, the first synthesis of **3** was reported by Sakurai et al. starting from *syn*-

119 benzotrinorbornadiene (**18**) [30] (Fig. 5b). Particularly advantageous is using the norbornadiene

120 scaffold, which contains two exploitable double bonds, thus one can be involved in the

cyclotrimerization process, the second can be used for further post-synthesis functionalization of the BCT scaffold.

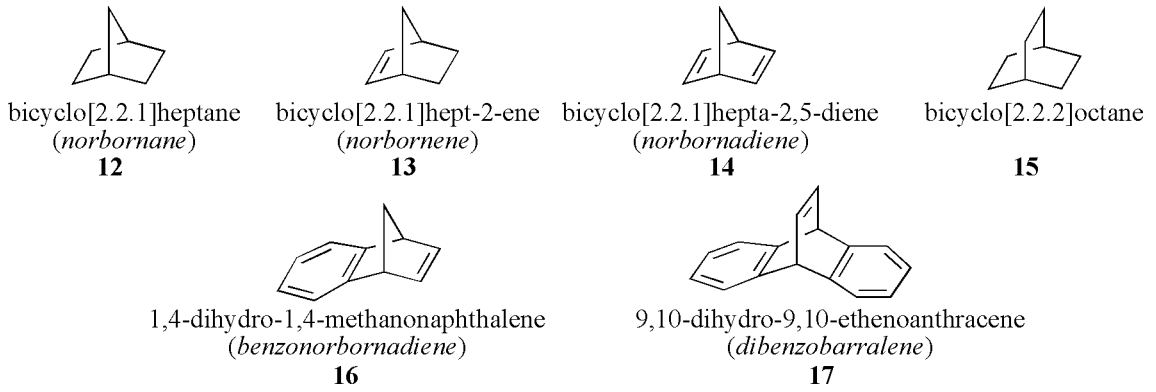

Fig. 4. Examples of bridged polycyclic hydrocarbons **12**-**17**.

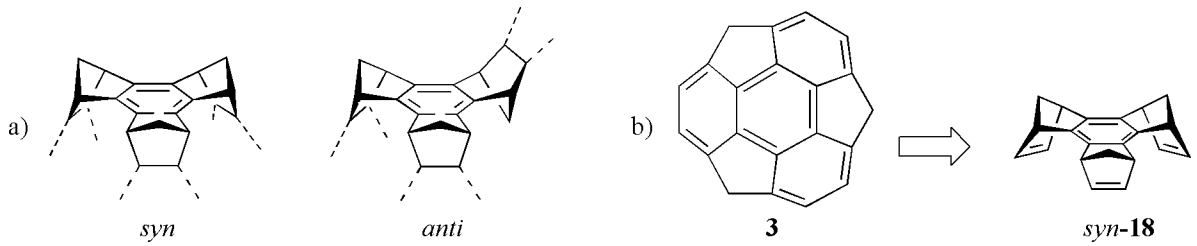

Fig. 5. a) *syn*- and *anti*-BCTs containing a bridged polycyclic motif; b) retrosynthetic scheme of Sakurai's synthesis of sumanene (**3**).

In 2011, the chemistry of bridged BCTs was briefly reviewed by Fabris *et al*. [20]. The aim of this comprehensive and updated review is to describe the evolution of the concept from the first simple bridged BCTs to the most recent gated molecular baskets developed as dynamic receptors for molecular delivery. Seminal studies and findings which have signed the bridged BCTs history will be examined and discussed in a timeline perspective: *a)* starting from the late 1960s, the isolation of BCTs obtained through cyclotrimerization of bridged polycyclic olefines was considered an evidence of the existence of strained acetylenes as reactive transient intermediates [31, 32]; *b)* at that time, a number of studies also focused on the chemo-physical features of BCTs, in particular on bond alternation observed in trisanellated benzenes due to the strain-induced bond localization in the central benzenoid ring (Mills-Nixon postulate) [33]; *c)* later, the potential of bridged polycyclic motifs to build concave receptors was

138 envisaged by Stoddart and co-authors [34, 35]; *d)* improvements in *syn*/*anti* diastereoselectivity have
139 allowed bridged BCTs to be prepared in moderate-high yields, becoming available for applications [36-
140 39]; *e)* bridged *syn*-BCTs have become privileged starting substrate for Sakurai's synthesis of
141 sumanenes [30]; *f)* finally, in the last few decades, concave bridged BCTs have been designed and
142 prepared by some groups as molecular containers for various applications, relevant developments in this
143 direction have been reported by Badjić's group [40, 41].

144 **2. A HISTORICAL OVERVIEW: DECADES 1960s-1990s**

145 In the beginning, products of cyclotrimerization of bridged polycyclic alkenes were considered of
146 interest as proof of the transitory formation of strained, and extremely reactive, alkynes such as the
147 bicyclo[2.2.1]hept-2-yne (**19**). The first reported bridged BCT was heptiptycene (**20**), obtained by
148 Huebner at al. in low and unspecified yield as a minor product from the reaction of 11-chloro-9,10-
149 dihydro-9,10-ethenoanthracene (**21**) with butyllithium (BuLi) (Fig. 6) [32].

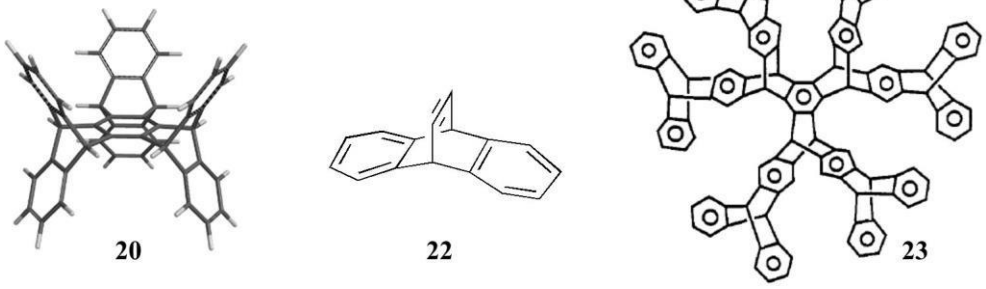

150150

151 **Fig. 6.** Structure of heptiptycene (**20**), bicycloalkyne **22**, and BCT **23** (adapted with permission from ref. 43).

152 In 1981, Hart at al. obtained **20** through lithiation of **21** in 20% yield [42], demonstrating the
153 formation, by lithium chloride elimination, of the bicycloalkyne **22** as a reactive species. With the same
154 methodology, the large BCT **23** was also obtained by Hart [43], but in very low yield (2%). In 1988,
155 Shahlai and Hart demonstrated that the bicyclo[2.2.2]octyne derivative **22**, generated from the 2-chloro-
156 3-lithiobicycloalkene **24**, undergoes stepwise reaction with additional two molecules of **24** providing the

lithiated trimer **25** which, after electrocyclization and LiCl elimination, gave the trimer **20** (Scheme 2) [36].

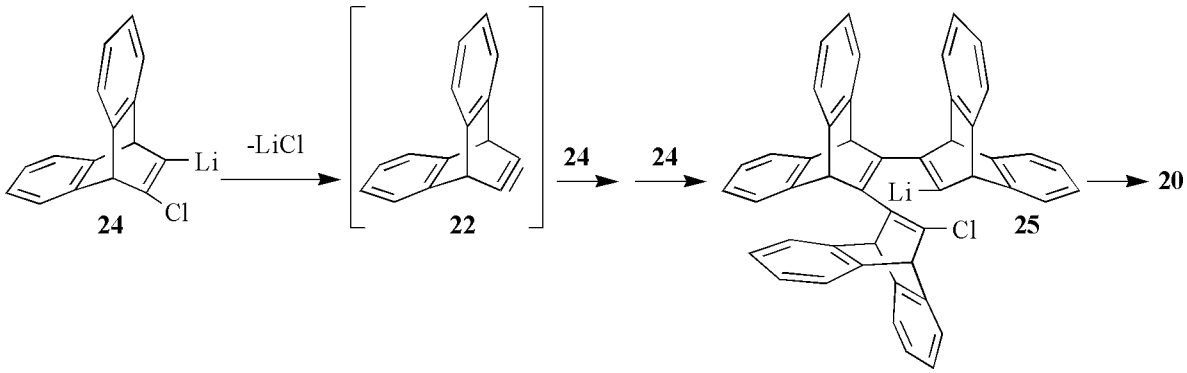

Scheme 2. Formation of **20** through stepwise cyclotrimerization of **24**.

On the other hand, in 1980 Gassman and Gennick obtained a 1 : 2 mixture of benzotrinorbornenes *syn*- and *anti*-**26** as a white solid (9-11% yield, m.p. 162-164 °C), along with an intractable gum, by heating of a solution of 2-lithio-3-chlorobicyclo[2.2.1]hept-2-ene (**27**) to 45 °C for 4 h (Scheme 3) [44].

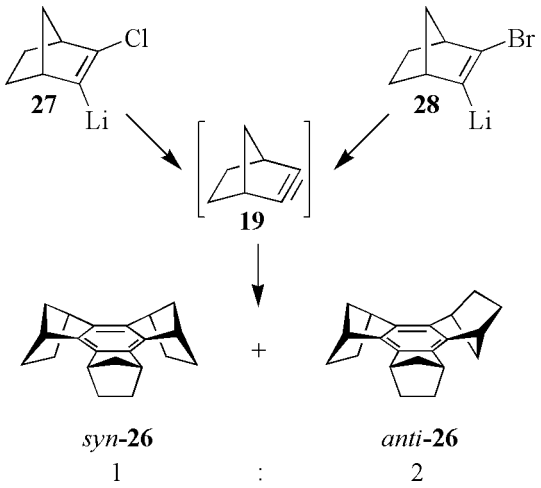

Scheme 3. Cyclotrimerization of **27** and **28** affording **26** through the transient formation of the alkyne **19**.

Analogously, treatment of a solution of 2-lithio-3-bromobicyclo[2.2.1]hept-2-ene (**28**) with bis(cyclopentadienyl)nickel (nickelocene) at low temperature, and successive warming to room temperature, furnished a mixture of *syn*- and *anti*-**26** in 37% yield. Interestingly, the bromo-substituted derivative **28** gave the BCT **26** when heated in the presence of nickelocene or other metal catalysts, but not when only heated. In all cases, the formation of **26** proceeded by cyclotrimerization of the transient strained alkyne **19** formed by elimination of lithium halide from the lithiated olefin.

In agreeement with the stepwise mechanism envisaged by Hart for the formation of **20** [36], in the 1980s Komatsu *et al*. found that treatment of 2,3-dibromobicyclo[2.2.2]oct-2-ene (**29**) with *n*-BuLi gave the dimer **30** through coupling of the strained alkyne **31** and the lithiated species **32** [45-47]. In the final steps, trimeric dibromide **33** provided D_{3h} benzocyclotrimer **34** in good yield (80.4%), after reductive cyclization (Scheme 4). Thus, despite the fact that the involvement of the alkyne **31** in the process was envisaged, as a matter of fact the BCT **34** was obtained not by direct cyclotrimerization of the acetylenic intermediate, but by reductive cyclization of the trimeric dibromide. The occurrence of a stepwise mechanism was demonstrated by the isolation of products of dimerization of **29** [47]. It is worth mentioning that the authors observed that the cyclotrimerization of **29** proceeded regardless of the presence of Ni(II) complexes, such as nickelocene or $Ni(PPh_3)_2Cl_2$, which had been erroneously believed to be active as a catalyst [46]. Referring to the alkyne-based mechanism described by Gassman [44], Komatsu noted that the more strained alkyne **19** may be supposed to undergo facile trimerization with itself, while for the less strained alkyne **31** a relatively longer lifetime makes the insertion of the triple bond into the C-Li bond possible [46].

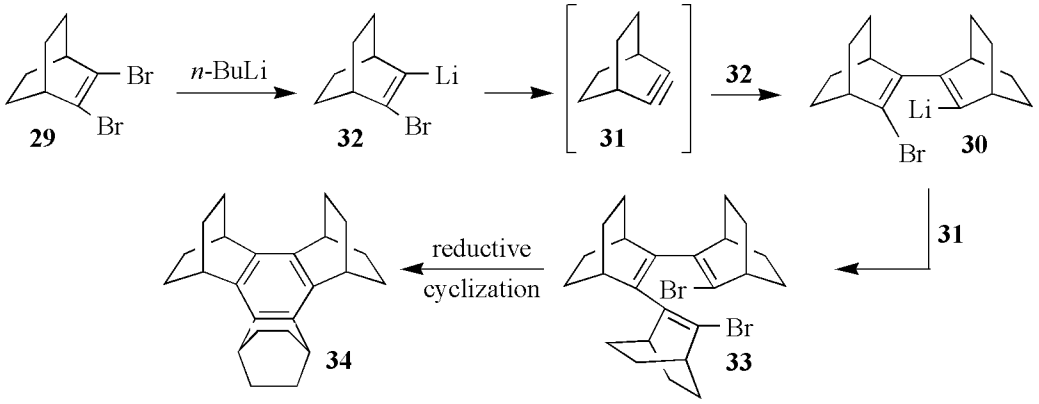

Scheme 4. Formation of **34** through stepwise cyclotrimerization of **29**.

In 1997, the same group synthesized two BCTs (**35** and **36**) containing two bicyclo[2.2.2]octene and one 7-oxa-bicyclo[2.2.1]hepta-2,5-diene moieties as branches (25% yield), through the transient formation of a bicyclo[2.2.2]octene-annelated benzyne **37** (Fig. 7) [48].

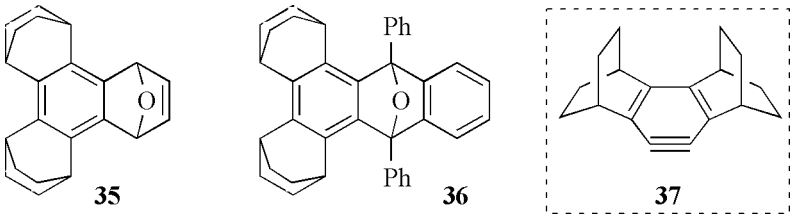

Fig. 7. Bridged BCTs **35** and **36**, and transient alkyne **37**.

In 1995, Siegel *et al*. synthesized the D_{3h} symmetric trisbicyclo[2.1.1]hexabenzene (**38**) starting from the bicyclo[2.1.1]hexan-2-one (**39**) which, under the conditions of the base-catalyzed elimination methodology of Wittig, afforded the 2,2-dichlorobicyclo[2.1.1]hexane (**40**), and then the 2-chlorobicyclo[2.1.1]hex-2-ene (**41**). The reaction mixture was then treated with a mixture of *tert*-BuLi and potassium *tert*-butoxide, followed by the addition of 10 mol% nickelocene to obtain, under the experimental condition reported by the authors, the BCT **38** in very low yield (< 1%) (Scheme 5) [49].

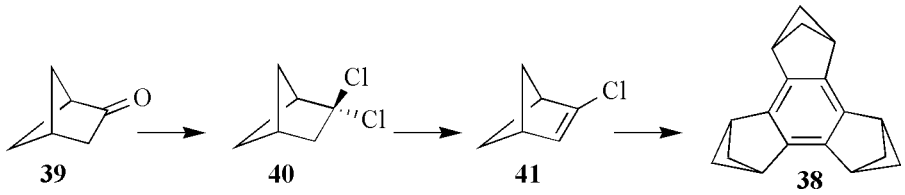

Scheme 5. Synthesis of **38** from the polycyclic ketone **39**.

In 1996, De Lucchi *et al*. obtained *syn*- and *anti*-**18** as an almost statistical mixture of isomers (1 : 2.6) in 10% yield, through cyclotrimerization of 2,3-dibromonorbornadiene (**42**) with BuLi and CuI [50]. The BCTs were characterized by NMR spectroscopy. The same procedure was applied to the cyclotrimerization of the alkene **43**, however in this case it was unsuccessful for the preparation of the corresponding BCT, whereas the dimers **44** and **45** were obtained exclusively (60% yield), which were characterized by diffractometric analysis (Scheme 6) [50]. Later, the same group reported the preparation of the benzotris(benzonorbornadiene) (**46**) by treating dibromobenzobornadiene (**47**) with *n*-BuLi at low temperature, followed by the addition of CuI [51]. A 1 : 2 mixture of *syn*- and *anti*-**46** was obtained (up to 50% yield), and the two isomers were characterized by NMR spectroscopy. The isomer *syn*-**46** was crystallized from acetone/water, and then characterized by diffractometric anaysis.

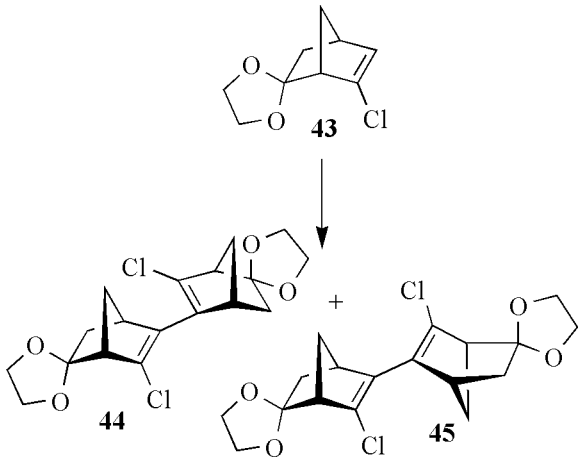

211211

212 **Scheme 6.** Dimerization of **43** affording dichlorodimers **44** and **45**.

213 By applying a procedure involving trimethylstannylalkenes developed to synthesize **46** [52], in 1999,
214 Fabris and De Lucchi reported the cyclotrimerization, with copper(II)nitrate trihydrate
215 ($Cu(NO_3)_2{\cdot}3H_2O$), of the bromotrimethylstannyl alkene **48** which was obtained from (+)-camphor (**49**)
216 in 64% yield. The cyclotrimerization reaction afforded a complex mixture of products containing both
217 *syn*- and *anti*-**50** in 5% and 45% yield, respectively (Scheme 7) [53].

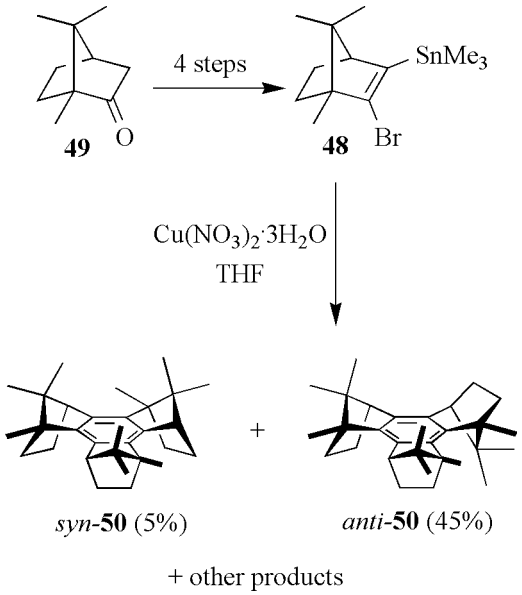

218218

219 **Scheme 7.** Cyclotrimerization of (+)-camphor (**49**) affording *syn*- and *anti*-**50**.

220 It is worth noting that structures and topologies synthesized in the decades 1960s-1990s, along with a
221 number of pioneering mechanistic findings, will have a pivotal role in the development of the field in the

years ahead, laying the bases for all successive studies, synthetic methods, and applications of bridged BCTs which have been developed so far.

3. MILLS-NIXON HYPOTHESIS: BOND LENGHT ALTERNATION IN ANNELATED BENZENES

To explain bond length alternation and the enhanced reaction selectivity observed in annelated benzenes, in 1930 Mills and Nixon hypothesized that the presence of small ring annelation onto a central benzene would induce significant bond length alternation within such benzene core [54-56]. This hypothesis was based on the existence of a tautomeric equilibrium of two Kekulé tautomers [55, 56]. However, current treatment of benzene as a single D_{6h} resonance hybrid, among a series of valence bond structures, instead of the result of a tautomeric equilibrium, weakens the conceptual bases of the Mills-Nixon explanation. The consequence of this incongruence, along with the fact that until 1980s there was no conclusive evidence of the Mills-Nixon effects, animated discussion on this explanation of double bond fixation in annelated benzenes [57-61]. Given that, an indicator which is frequently used to evaluate the magnitude of bond length alternation is the difference between the *endo* and *exo* carbon-carbon bond length of annelated benzenes, namely $\Delta r = r_{endo} - r_{exo}$, which can be determined computationally and experimentally (Fig. 8a) [56].

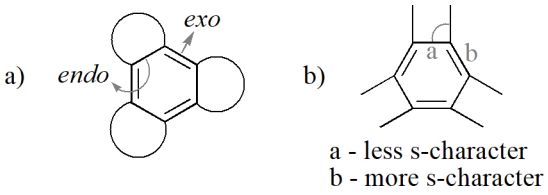

Fig. 8. a) Position of the double bonds in (*endo*) or out (*exo*) the annelated ring; b) the σ-strain induced re-hybridization effect.

The bonding character of the molecule can be also evaluated, and two concurrent mechanisms have been envisaged: *a)* the *σ-strain effect*, which causes re-hybridization in the strained atoms (Fig. 8b). Indeed, due to the repulsion between the *endo* carbon-carbon bond and the bonds of the annelated small rings, the atoms of the central benzene are not sp^2-hybridized, but have a different hybridization at each

of the bond directions. On this basis, the *endo* bond has a higher p-character in order to reduce the strain caused by the annelated ring, whereas the hybrid orbital in the *exo* direction has a higher s-character. Thus, the *exo* bond is shorter than the *endo* one, with a positive Δr [56,58]; *b)* the π-effect which is based on the aromaticity and antiaromaticity concepts [61], and in this case the carbon-carbon bonds in the central ring are alternate to avoid the anti-aromatic destabilization.

Despite the controversy about the reliability of the Mills-Nixon hypothesis, bond fixation have occurred in many annelated benzenes, and over time it was evaluated both experimentally and computationally, the entity of the phenomenon being rather variable [55, 62, 63]. On the other hand, the possibility to use small strained rings to induce bond alternation has been considered attractive because electron localization in aromatic systems may lead to new tools to modulate chemical reactivity [64]. For instance, Kochi *et al*. noted that the structural modification of benzene with a bicycloalkane framework leads to the remarkably stabilization of reactive intermediates associated with electrophilic aromatic substitution, such as the Wheland intermediates [65] and cation radicals [66].

In 1995, Burgi, Siegel *et al*. analyzed the structure of **20** for bond alternation in the central benzene ring as a function of annelating substituents [67]. The central ring of heptiptycene was found to be essentially planar, and average lengths of the two constitutionally different carbon-carbon bonds in the central ring differed by Δr = 0.022(9) Å. The authors compared the experimental structure with geometries calculated at Hartree-Fock (HF) and density functional theory (DFT) levels, which confirmed almost no bond localization within the central ring due to a rather low extent of bond alternation. For BCT **34**, Komatsu's group found by X-ray diffractometric analysis that the aromatic bond lengths alternate slightly, with average bond length of 1.408 Å and 1.393 Å in and out of the bicyclic systems, respectively (Δr = 0.015 Å) [45]. Higher degree of bond alternation was observed by Siegel *et al*. for the more strained C_{3v} symmetrical BCT *syn*-**26** through calculations, with *endo*/*exo* bond lengths of 1.416/1.364 Å (HF) (Δr = 0.052 Å) and 1.415/1.374 Å (DFT) (Δr = 0.041 Å), and experimentally with average *endo*/*exo* bond lengths of 1.417(2)/1.379(2) Å (Δr = 0.038 Å) [68]. On the

basis of the evidence of bond localization in *syn*-**26**, the authors analyzed the barrier to rotation about the metalarene bond in the *syn*-**26**-Cr-$(CO)_3$ complex (Fig. 9) [68, 69]. In the crystal, *syn*-**26**-Cr-$(CO)_3$ adopts a conformation controlled by avoiding the steric overlap (complex-I, **51**), in which the Cr-carbonyl bonds eclipse the *exo* bonds of *syn*-**26**, thus being far from the proximal alkyl bridges. Rotation about the metal-arene bond by 60° (complex-II, **52**) maximizes the steric congestion between alkyl bridges and the carbonyls but offers a better ligand field arrangement (octahedral). The energy contribution coming from the ligand field arrangement has been quantitatively correlated to the magnitude of the bond alternation in the uncomplexed arene [68, 70].

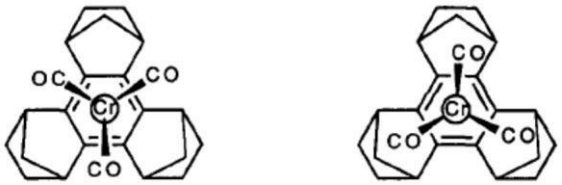

26-$Cr(CO)_3$-I (**51**) **26**-$Cr(CO)_3$-II (**52**)

Fig. 9. Structures of complexes **26**-Cr(CO)3-I (**51**) and –II (**52**) (adapted with permission from ref. 68).

BCT **38** shows a unique type of strained annelation of benzene. In 1992, Siegel *et al*. reported *ab initio* calculations at the restricted HF/6-31G(D) and density functional theory (DFT) levels, predicting a large bond alternation for **38**, with *endo*/*exo* bond lengths of 1.440/1.344 Å (HF) (Δr = 0.096 Å) and 1.429/1.366 Å (DFT) (Δr = 0.063 Å) [33]. Later, the same authors performed the X-ray crystallographic analysis of **38** producing a structure consistent with the computational prediction, and observing two inequivalent bonds in the benzene ring with *endo*/*exo* bond lengths of 1.438(5)/1.349(6) Å (Δr = 0.089 Å) [60]. Recently, Chen et al. investigated the factors that may cause bond length alternation and π-bond localization in annelated benzenes, among them BCT **38**, performing *ab initio* valence bond calculation [56]. According with Siegel [55], the authors showed that the bond length alternation of annelated benzene is determined by the strain-induced hybridization change from equal bond length geometry to the equilibrium geometry. Both σ-strain and π–π interaction can cause bond length alternation. The σ-

strain always lengthening the *endo*-bond but shortens the *exo*-bond, leading to a positive Δ*r* value. Moreover, molecules such as **38** were shown to exhibit π–π repulsion between the annelated and the central rings, which induce distorsion of the bond length in the positive Δ*r* direction.

Kohnke, Stoddart *et al*. prepared BCT **53** consisting of benzene fused to three 2,5-dihydrofuran residues (Fig. 10) [34, 35], finding significant bond localization in the benzene ring with average *endo*/*exo* bond lengths of 1.425(7)/1.353(6) Å (Δ*r* = 0.072 Å) [71].

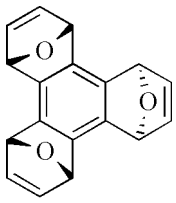

anti-**53**

Fig. 10. Structure of *anti*-**53**.

From the examples reported in this section, it appears evident that the ring size of the polycyclic system impacts the extent of ring strain and, consequently, of bond fixation. BCT **38** and **53** are the most strained, producing an experimental Δ*r* = 0.089 and 0.072 Å, respectively. Adding a carbon atom to the bicyclic ring obtaining **26** reduces the strain, with Δ*r* = 0.038 Å. Less strained systems such as **20** and **34** behave almost as normal aromatic rings with Δ*r* = 0.022 and 0.015 Å, respectively.

4. SYNTHESIS AND TRANSFORMATION OF BRIDGED BCTs: THE *SYN*/*ANTI* STEREOSELECTIVITY ISSUE

In general, the application of metal-catalyzed cyclotrimerization [72] of highly strained and transient alkynes, such as **19** and **31**, to synthesize bridged BCTs led to unpredictable results and low yields [44, 49]. Thus, the most efforts from chemists converged on the cyclotrimerization of stable alkenes through metal-catalyzed coupling reactions, $R^{\delta+}$-X + R'$^{\delta-}$-Y → R-R', which proved to be fruitfully applicable to the synthesis of annellated benzenes decorated with bridged polycyclic motifs in good yields. Over time, the most methodologies have focused on the possibility to obtain stereoselectively

syn-BCTs which are featured by concave topologies, and thus attractive to develop new molecular containers.

4.1. Possible stereochemical pathways in cyclotrimerization of polycyclic alkenes

Given the formation of BCT **18** as an example, in principle the selective production of the *syn*-isomer may occur through a chain-coupling mechanism (Fig. 11a) starting from an enantiopure alkene **54** properly functionalized. Otherwise, given the cyclotrimerization occurring *via* formation of a strained alkyne **55**, *in situ* formed during the process (Fig. 11b), a statistical 1 : 3 mixture of *syn*/*anti* isomers would be expected whatever the stereochemistry of **54**, provided that the rates of competing reaction pathways are comparable.

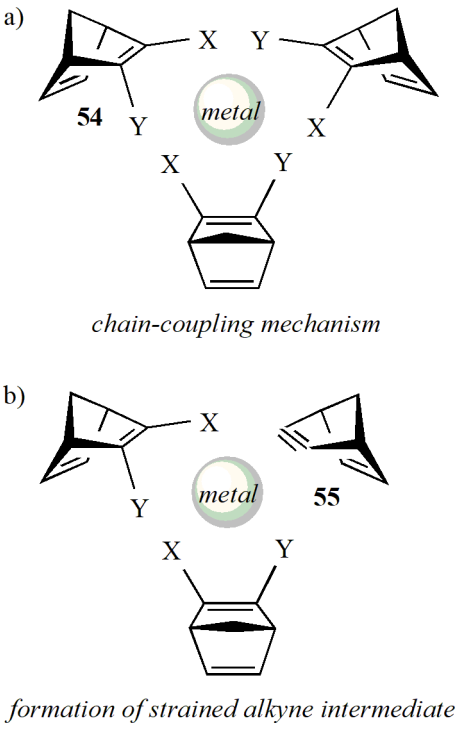

Fig. 11. Possible cyclotrimerization mechanisms of alkene **54** to BCT **18**.

Indeed, despite the fact that BCT **18** is not chiral, *syn*- and *anti*-isomers being C_{3v} and C_s molecules, respectively, the stereochemistry of the chiral starting alkene **54** may play a key role in determining the cyclotrimerization outcome. In the perspective of a chain-coupling mechanism, while the *syn*-isomer would be formed through successive homochiral couplings of enantiopure units of **54**, the use of *rac*-**54**

would provide the statistical 1 : 3 mixture, derived by the statistical occurrence of both homochiral and heterochiral couplings (Scheme 8) at comparable rates. This process appears stereochemically analogous to the base-promoted steroselective aldol self-coupling of racemic norbornenones reported by Paquette [73].

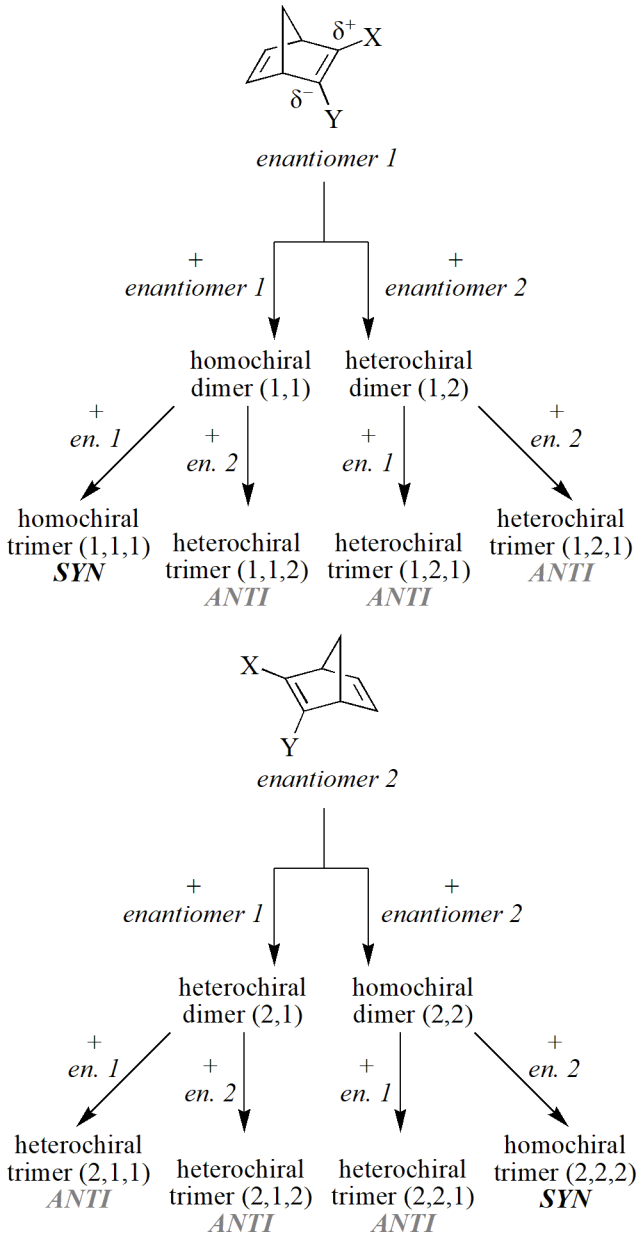

Scheme 8. Scheme of the stereochemical couplings of the enantiomers of chiral alkene **54** producing the 3: 1 statistical distribution of *syn* and *anti* BCTs.

It is worth mentioning that the chiral information, contained in the starting alkene **54** at the two bridgehead carbon atoms, is lost in the symmetric alkyne **55** which, consequently, also would determine

the statistical distribution of the resulting BCTs. The possibility of stepwise processes, occurring through the formation of open dimers and trimers, were observed by Hart [36, 42] and Komatsu [47] during the synthesis of the BCTs **20** and **34**, respectively, even if in this cases cyclotrimerization was supposed to occurr *via* formation of strained alkynes.

4.2. Synthesis of bridged BCTs from polycyclic alkenes

The peculiarity of the coupling reaction of polycyclic alkenes affording bridged BCTs is that electrophile ($R^{\delta+}$-X) and nucleophile ($R'^{\delta-}$-Y) sites are located in the same molecule which, consequently, presents two vicinal carbon atoms with opposite polarization (Scheme 8). Metal-catalyzed cyclotrimerisation processes involving this type of double polarized alkenes proceed through mechanisms involving metalated alkene units and diastereomeric metal complexes. In the late 20th century, Ni-mediated cyclotrimerization of polycyclic alkenes were explored by several groups but with poor results in terms of isolated yields of BCTs [45, 47]. Otherwise, coupling reactions promoted by stechiometric amount of copper salts and those catalyzed by palladium catalysts have been allowed bridged BCTs to be successfully synthesized for several years. Under metal-mediated conditions, stereochemical pathway and outcome of the process are expected to be governed by nature and properties of the metal, complex geometry, solvent, and other additives modulating the catalytic activity [37, 39, 74]. Thus, by selecting properly experimental conditions, a single stereochemical pathway may become favoured and, depending of the structure of the starting alkene, the diastereomeric distribution of the final BCT products may go beyond the statistical value.

4.2.1 Synthesis of bridged BCTs through copper-promoted cyclotrimerization

As mentioned in section 2, in the late 1990s De Lucchi *et al*. obtained BCTs, in moderate yields and statistical *syn*/*anti* ratio, by using the metallic system *n*-BuLi/CuI [50,51]. Later, the same group performed intensive studies on coupling reactions involving bridged polycyclic alkenes containing the trimethylstannyl group as 'metal' and bromine as leaving group [52, 75, 76]. The trimethyltin moiety could be introduced starting from *vic*-dibromoalkenes by metal-halogen exchange with *n*-BuLi followed

by trans-metalation with trimethyltin chloride. Alternatively, bromoalkenes afforded trimethylstannyl derivatives by deprotonation with lithium diisopropylamide and subsequent quenching with trimethyltin chloride. On this basis, starting from 2,3-dibromonorbornene (**56**), 2,3-dibromonorbornadiene (**57**), and **47** with *n*-BuLi in THF, followed by treatment with trimethyltin chloride, De Lucchi's group prepared the corresponding 2-bromo-3-trimethylstannyl derivatives **58**-**60** [52, 75]. This procedure was successful improved for derivative **60** which was prepared by direct lithiation and transmetallation of 2-bromobenzonorbornadiene (**61**) (Scheme 9).

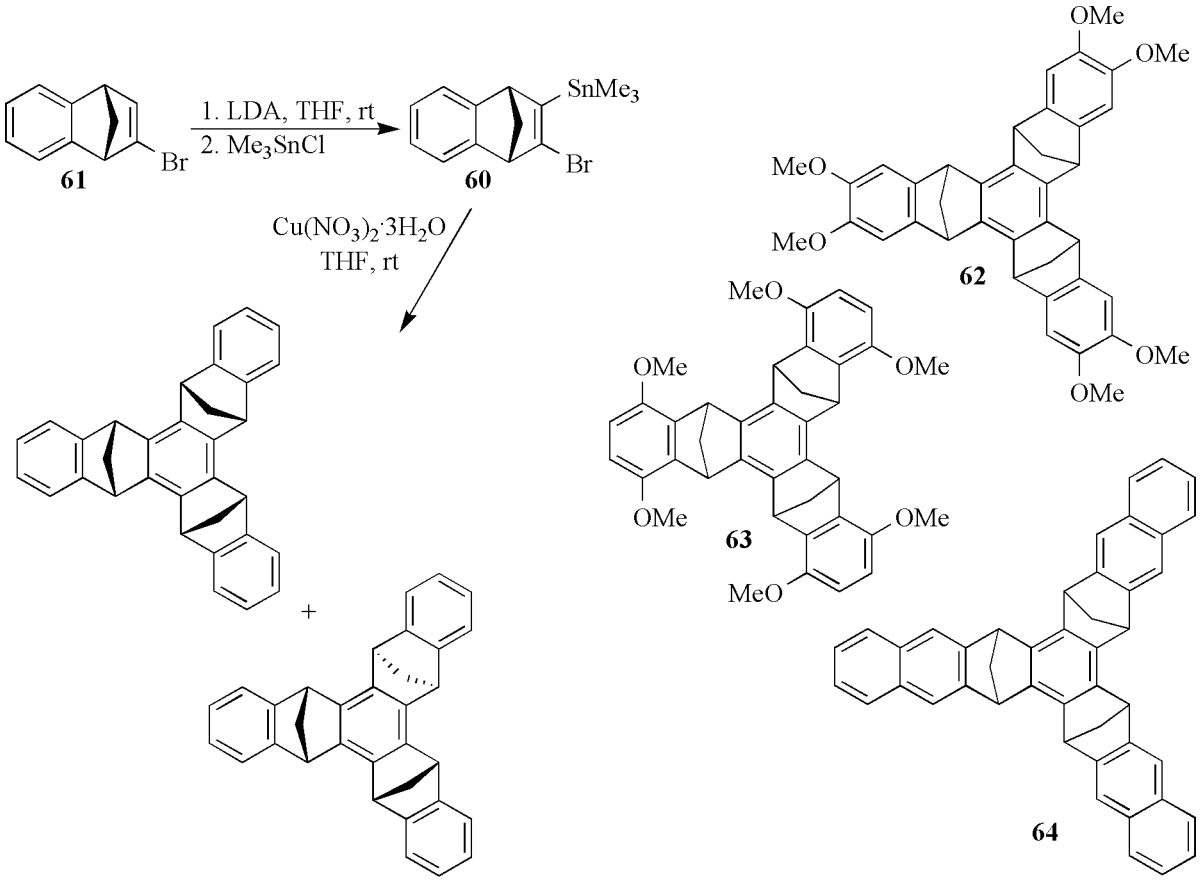

Scheme 9. Preparation of **60** from **61**, and cyclotrimerization of **60** affording BCTs **46**. Structures of BCTs **62**-**64**.

Then, the cyclotrimerizations of derivative **58**-**60** were performed with a stechiometric amount of $Cu(NO_3)_2{\cdot}3H_2O$, obtaining BCTs **18**, **26** and **46** as statistical mixtures of *syn*/*anti* isomer, but in yields up to 80% [52, 75, 76]. In Scheme 9, the reaction is summarized for BCT **46**. The cyclotrimerization was shown to be unsuccessful by using other copper salts such as CuCl and CuI_2, and different metal

promoters such as iron(III) chloride and Pd^0 [75]. By applying the methodology based on the use of $Cu(NO_3)_2 \cdot 3H_2O$ as a coupling-promoter, other benzotris(benzonorbornadiene)s such as the 5,8- and 6,7-dimethoxy BCTs **62** and **63**, and the naphtho-substituted BCT **64** were also prepared by the group in yields ranging from 15% to 47% [76]. The cyclotrimerization performed starting from the enantiopure **60** afforded *anti*-**46** (yield 62%), along with a minor amount of *syn*-**46** (3%), a protodestannylated product **65** (10%), and the two diastereomeric dimers *anti*-**66** (17%) and *syn*-**66** (3%) (Fig. 12), derived from homochiral and heterochiral coupling of the starting monomers, respectively [52].

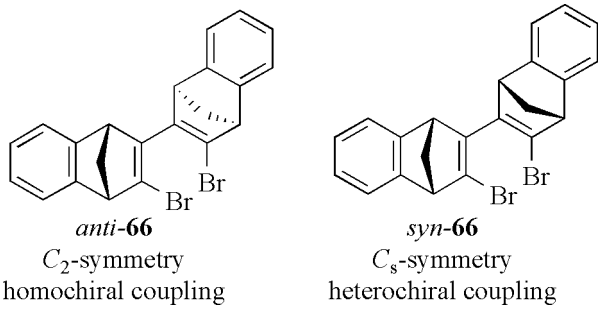

Fig. 12. Structures of the brominated dimers **66** formed in cyclotrimerization of enantiopure **60**.

De Lucchi and co-authors explained the formation of the trimer *anti*-**46** as driven from the occurrence of a Sn-Sn coupling to form the dimer *anti*-**66** followed by a Br-Sn exchange performed by a tin-copper species to form the metalated *anti*-**67** (Scheme 10).

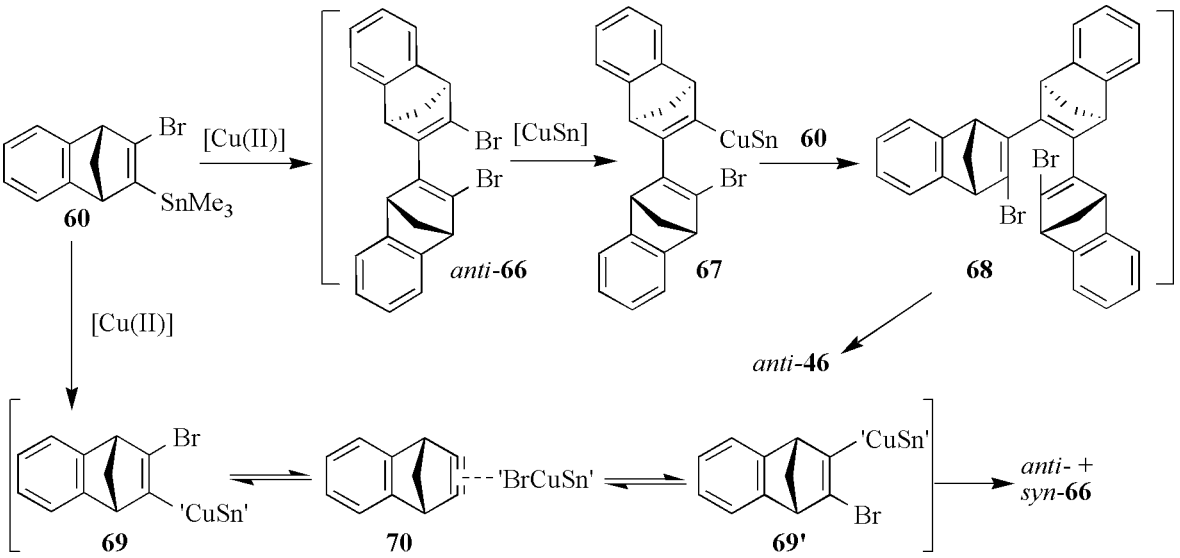

Scheme 10. Proposed mechanism for the cyclotrimerization of enantiopure **60** promoted by $Cu(NO_3)_2 \cdot 3H_2O$.

The addition of the third unit of **60** was hypothesized to provide the open trimer **68** which, analogously to the intermediate **33** reported by Komatsu [47], gave spontaneous cyclization affording *anti*-**46**. The formation of minor quantities of *syn*-**66** was explained though the formation of the dimer *syn*-**69** as a product of heterochiral coupling occurring after a racemization process of the enantiopure monomer through formation of the alkyne intermediate **70**.

Starting from the conditions reported by Piers for CuCl-mediated homocoupling of alkenyltrimethylstannane [77], in 2001 Cossu *et al*. described the first direct access to *syn*-**46** starting from *rac*-**60** by using CuI as a copper salt, and the optimized conditions reported in Table 1 (Entry 10, highlighted in grey) [37].

Table 1. Reagent, solvents, reaction conditions, products and yields for cyclotrimerization of **60**.

Entry	CuX	Solvent	Cosolvent	LiX	T (°C)	*t* [h]	*syn*/*anti*-**46** (yield%)	*syn*- + *anti*-**66** [%]
1	CuCl	DMF	--	--	rt	1	1 : 2 (75)	traces
2	CuCl	THF	--	LiCl	rt	4	1 : 2 (5)	5
3	CuCl	DMF	--	LiCl	rt	19	1 : 1 (50)	50
4	CuCl	DMF	DME	LiCl	60	4	2 : 1 (80)	--
5	CuCl	DMF	DMDPE	LiCl	rt	2	2 : 1 (70)	20
6	CuI	DMF	DME	LiCl	rt	24	4.5 : 1 (80)	3
7	CuI	DMF	DME	LiBr	rt	360	3 : 1 (15)	35
8	CuCl	DMF	DME	LiI	rt	168	1 : 1.5 (25)	25
9	CuI	DMF	DME	LiI	rt	12	--	--
10	CuI	NMP	DME	$LiNO_3$	rt	24	9 : 1 (80)	--

DMF = *N*,*N*-dimethylformamide; DME = 1,2-dimethoxyethane; DMDPE = *rac*-1,2-dimethoxy-1,2-diphenylethane; NMP = *N*-methylpyrrolidinone; THF = tetrahydrofuran.

Applying the optimized conditions (Table 1, Entry 10), **64** was obtained with 9:1 *syn*-*anti* ratio, **62** as *syn*-isomer exclusively, whereas these conditions proved to be unsuccessful for synthesis of BCTs **63** and **18**. Moreover, the reaction of enantiopure **60** was dramatically slower than that of *rac*-**60** affording traces of *anti*-**46** exclusively. These results as well as the formation of dimers **66**, observed in some cases (Table 1, entries 1-3 and 5-8), suggested *a*) the occurrence of a Sn-Sn coupling process, *b*) an intrinsic reluctance of homochiral monomers to couple between themselves, and *c*) that the reaction cannot proceed via a symmetric alkyne metal complex in which the chiral information would have been lost.

Thus, starting from the racemic alkenes, the mechanism was supposed to proceed with a total selectivity of each enantiomer in choosing the reaction partner of opposite configuration, not only in the formation of the dimer, but also in the further coupling evolving to the trimer formation (Scheme 11a) [37].

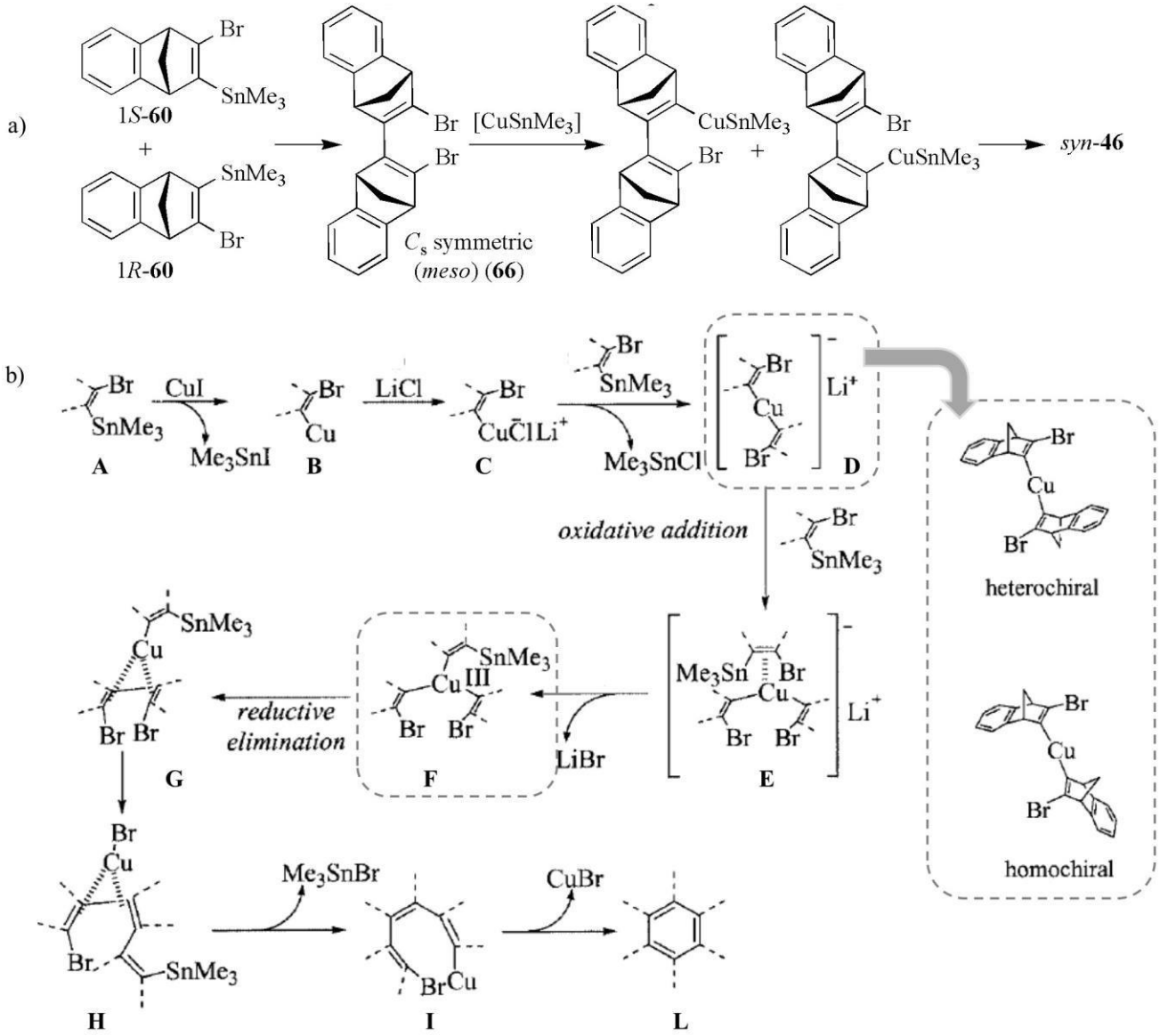

Scheme 11. Mechanism of CuI-mediated cyclotrimerization of *rac*-**60** affording *syn*-**46** stereoselectively (adapted with permission from ref. 78).

Later, a carefully evaluation of the chemical properties of the species involved in the process allowed the authors to reasonably explain the stereoselective formation of the *syn* isomer through a ligand

coupling process fundamentally involving the participation of different diastereoisomeric metal complexes, in which the monomers are ligands of a central metal ion: under these conditions, the stereochemical pathway and, consequently, the stereochemical outcome are governed by both the nature and the property of metal and associated complex geometry [78]. This mechanism being summarized in Scheme 11b, stereochemically the process appears to be driven by the stereoselective formation of the heterochiral organolithium cuprate **D** and of the Cu(III) complex **F**, where three units of polycyclic alkenes assemble stereoselectively around the metal centre.

Copper-promoted cyclotrimerizations have showed to be substrate-dependent in terms of *syn*-stereoselectivity, product yields, and fine mechanisms. Starting from the bromotrimethylstannyl alkene *rac*-**71**, very recently Badjić *et al*. applied the CuI-mediated cyclotrimerization to the synthesis of BCT *syn*-**72** (Scheme 12) [79, 80], obtaining the desired BCT in 24% yield, albeit with 61% of undesired *anti*-**72**.

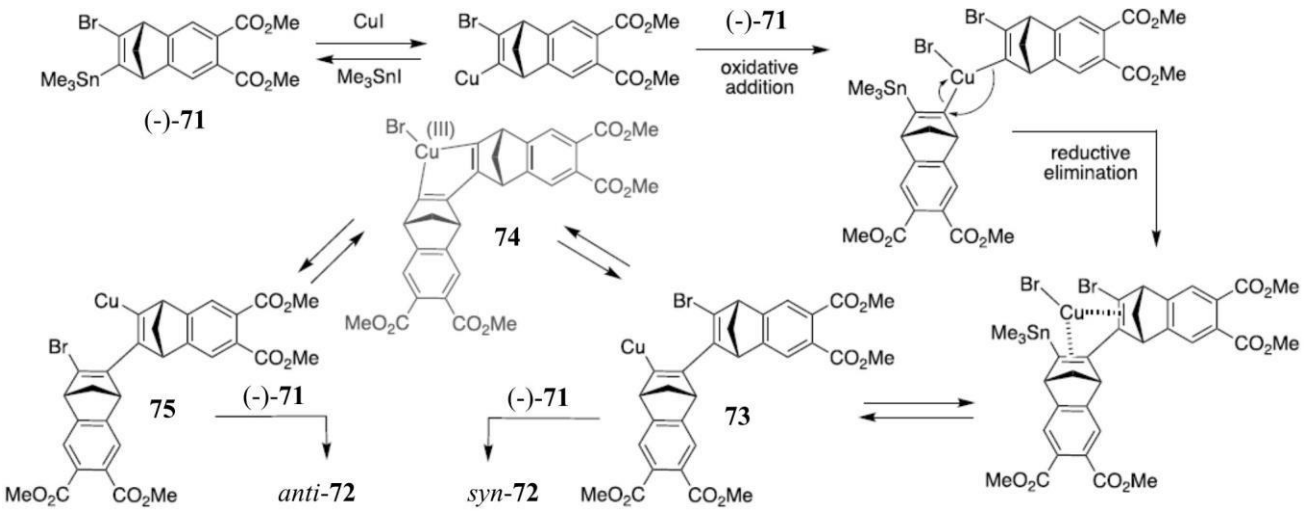

Scheme 12. Mechanism of CuI-mediated cyclotrimerization of *rac*-**71** affording *syn*-and *anti*-**72** (adapted with permission from ref. 80).

The authors also examined the CuI-promoted cyclotrimerization of enantioenriched (−)-**71** (96% ee) which was found to give BCT **72** in 1:1 *syn*/*anti* ratio (85% yield). Reducing the enantiopurity of (−)-**71** was found to have a steady and adverse effect on the quantity of the desired *syn*-diastereomer formed in the process. In this studies, the reaction were carried out at different temperature, and a chain-type

mechanism for the CuI-promoted cyclotrimerization of enantiopure (−)-**71** was envisaged by the authors, with the dimer **73** undergoing intramolecular oxidative addition to give achiral (*meso*) Cu(III) intermediate **74**, which after a reductive elimination may form enantiomeric **75** (Scheme 12).

In 2001, Matsuura and Komatsu carried out an efficient route to **38** by cyclotrimerization of the organometal derived from 2,3-diiodobicyclo[2.1.1]hex-2-ene (**76**), which was synthesized from **39** [81]. Indeed, treatment of the diiodoolefin **76** with *n*-BuLi in THF, followed by the sequential addition of CuI and $CuCl_2$, successfully afforded annelated benzene **38** in 21% yield (overall yield from **39**).

In 2002, Lucchini and co-authors used copper(I) thiophen-2-carboxylate (CuTC) in the cyclotrimerization of *rac*-[2.2.1]bicyclic *vic*-bromotrimethyltin olefins **48**, **59**, **77**, and **78** under the condition summarized in Table 2, obtaining high yields of *syn*/*anti* mixture of the corresponding BCTs [82]. The two diastereoisomers came in different ratios, smaller than or equal to the statistical 1 : 3 ratio depending on the steric hindrance opposed by the functionalities. CuTC as a promoter had been introduced in the late 1990s by Liebeskind [83, 84]. This species offers practical advantages being inexpensive, air stable, and nonhygroscopic, mediating the selective couplings between vinyl bromides and trialkylvinylstannanes and providing coniugated dienes in almost quatitative yields [84].

Table 2. Results of the cyclotrimerization reactions of alkenes **48**, **59**, **77** and **78** with CuTC and other copper salts.

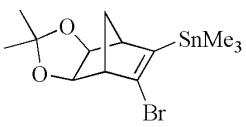

77

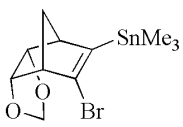

78

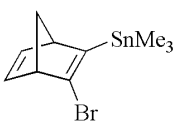

59

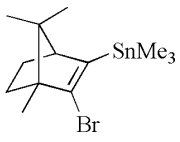

48

Substrate	CuX	Solvent	*t* [min]	T (°C)	*syn*/*anti* yield%)	protodestannylated reagent (%)	% C_s and C_2 dibromo-dimers
77	$Cu(NO_3)_2 3H_2O$	THF	20	25	1 : 4 (10)	70	20
77	CuI/LiCl	DME/DMF	24 h	25	--	--	--
77	'$CuNO_3$'	DME/DMF	20	-15	1 : 4 (70)	--	30
77	CuTC	NMP	20	-15	1 : 4 (98)	--	--
78	CuTC	NMP	12 h	-15 →25	1 : 8 (70)	--	--
59	$Cu(NO_3)_2 3H_2O$	THF	25	25	1 : 3 (78)	--	--

59	CuTC	NMP	25	-20	1 : 3 (94)	--	--
48	$Cu(NO_3)_2 \cdot 3H_2O$	THF	25	25	1 : 9 (50)	20	20
48	CuTC	NMP	40	-20	1 : 6 (98)	--	--

In early 2000, Fabris *et al*. explored the effects of different copper(I) and -(II) in the cyclotrimerization of enantiopure *vic*-bromo(trimethylstannyl)bicycloalkenes derived from (+)-camphor, (+)-fenchocamphorone, and (-)-epicamphor [53, 85]. Remarkably, in 2003 the authors prepared the (+)-*syn*-benzotriborneol (**79**) by CuTC-promoted cyclotrimerization, obtaining the BCT with high yield and *syn*-stereoselectivity [86]. Later, the chiroptical properties of benzotricamphor derivatives featured by different degrees of flexibility were studied as models to compare experimental and theoretical electronic circular dichroism (ECD) spectra [87].

In 2003, Sakurai's group also applied the CuTC-mediated cyclotrimerization of **59** to obtain *syn*-**18** as intermediate in sumanene synthesis (Scheme 13) [30]. Starting from the BCT *syn*-**18**, the authors explored the alkene-bridge exchange by the Ru-catalyzed tandem ring opening metathesis (ROM) and ring-closing metathesis (RCM) reaction. Thus, *syn*-**18** was treated with 10 mol% of $Cl_2(PCy_3)_2Ru{=}CHPh$ in toluene at 0°C, and then at room temperature under an atmospheric pressure of ethylene, giving **80** in 30% yield. Otherwise, tandem ROM-RCM reaction did not proceed from *anti*-**18**. Compound **80** was oxidized by dichlorodicyanoquinone (DDQ) to give sumanene in 70% yield.

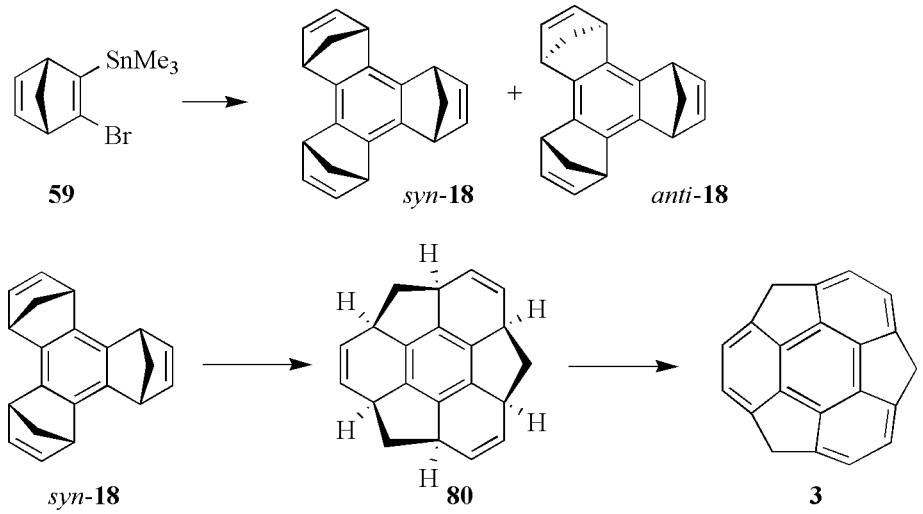

Scheme 13. Sakurai's synthesis of sumanene.

Later, a series of highly functionalized BCTs were synthesized through the CuTC-mediated cyclotrimerization. In particular, it was noted that the statistical 1 : 3 *syn* to *anti* ratio is frequently even

more in favour of the *anti* isomer because of the steric hindrance exerted by the three 'arms' of the BCT. On this basis, *syn* trimers with long and functionalized 'arms', which appeared the most interesting host molecules, were often generated in negligible quantity with respect to the *anti* isomers. Given that, some authors have tackled this issue by synthesizing *syn*-BCTs with short 'arms' which are decorated with groups allowing further functionalization [88] (Scheme 14). A first approach is based on the preparation of BCTs bearing reactive double bonds toward dienophile species. In 2003, Lucchini *et al*. performed the synthesis of the tris-annelated benzene **81** by cyclotrimerization of the monomer **82** [88]. Early attempts with the $Cu(NO_3)_2 \cdot 3H_2O$ as a promoter had failed, leading to the formation of complex mixtures of products including the protodestannylated monomer, and both C_s and C_2 dibrominated dimers. Otherwise, the reaction promoted by a stechiometric amount of CuTC allowed for obtaining a 1:4 mixture of *syn* and *anti* BCTs in almost quantitative yield (Scheme 14a) [88]. The isomers were separated by chromatography and recrystallized from methanol. Moreover, the Diels–Alder reactivity of *syn*-**81** was tested toward strong dienophiles, as tetracyanoethylene, dimethylacetylene dicarboxylate (DMAD), 4-phenyl-1,2,4-triazoline-3,5-dione (PTAD), and norbornadiene, affording *syn*-**83**-**86** in yields ranging from 50 to 100%. Later, Fabris, Daştan, *et al*. also obtained BCTs **87** and **88** after cyclotrimerization of alkenes **89** and **90**, respectively, with CuTC in dry NMP at -20 °C [89]. For **87**, the *syn* to *anti* diastereoselectivity and the yields of the products reflect the steric hindrance of the substituents (Scheme 14b). Indeed, alkene **89** furnished a 1 : 9 *syn* to *anti* mixture of BCT **87**, this unfavorable diastereomeric ratio being imputable by the authors to the steric repulsion between the carboxymethyl moieties acting on the plane of the ethylidene fragment of the bicycle. More striking resulted the effect of the alkene **90**, and in this case the *anti*-BCT **88** was obtained exclusively (Scheme 14c) [89]. In 2006, Badjić *et al*. performed the CuTC-promoted cyclotrimerization of polyene **82** obtaining **81** as a 4:1 mixture of *anti* and *syn* isomers in 65% isolated yield [90]. Compound **81** being highly reactive in Diels-Alder reactions [88], the cycloaddition of DMAD to **81** was performed at a high pressure in order to yield **91**, after the DDQ aromatization step (Scheme 14d).

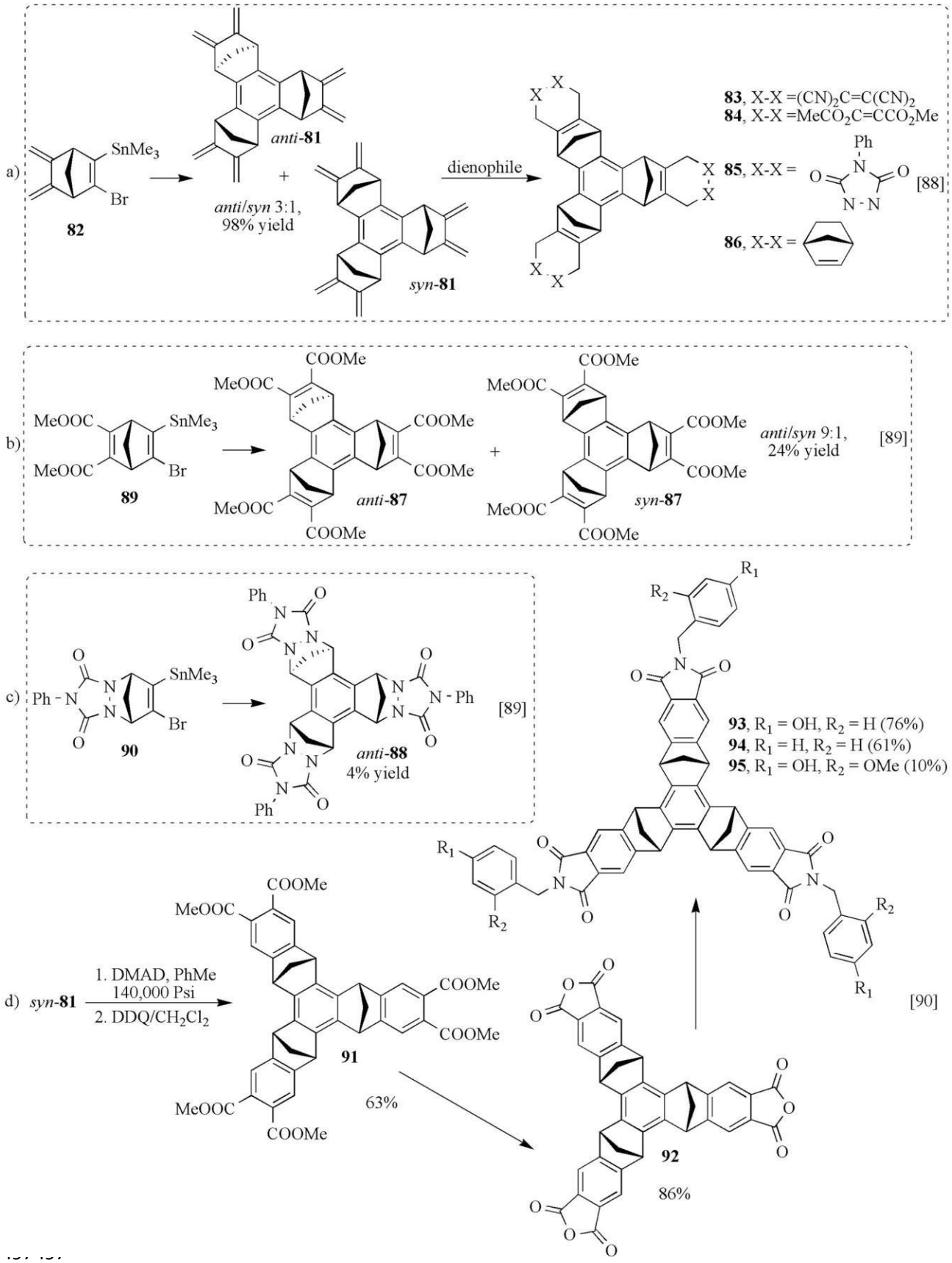
a)
SnMe3
Br
82
anti-81
+
anti/syn 3:1,
98% yield
syn-81
dienophile
83, X-X =(CN)2C=C(CN)2
84, X-X =MeCO2C=CCO2Me
85, X-X =
[88]
86, X-X =
b)
MeOOC
SnMe3
Br
89
COOMe
anti-87
syn-87
anti/syn 9:1,
24% yield
[89]
c)
Ph
SnMe3
Br
90
anti-88
4% yield
[89]
93, R1 = OH, R2 = H (76%)
94, R1 = H, R2 = H (61%)
95, R1 = OH, R2 = OMe (10%)
d) syn-81
1. DMAD, PhMe
140,000 Psi
2. DDQ/CH2Cl2
91
63%
92
86%
[90]

Scheme 14. CuTC-mediated cyclotrimerization of polycyclic alkenes affording BTCs and related derivatives (*continues*).

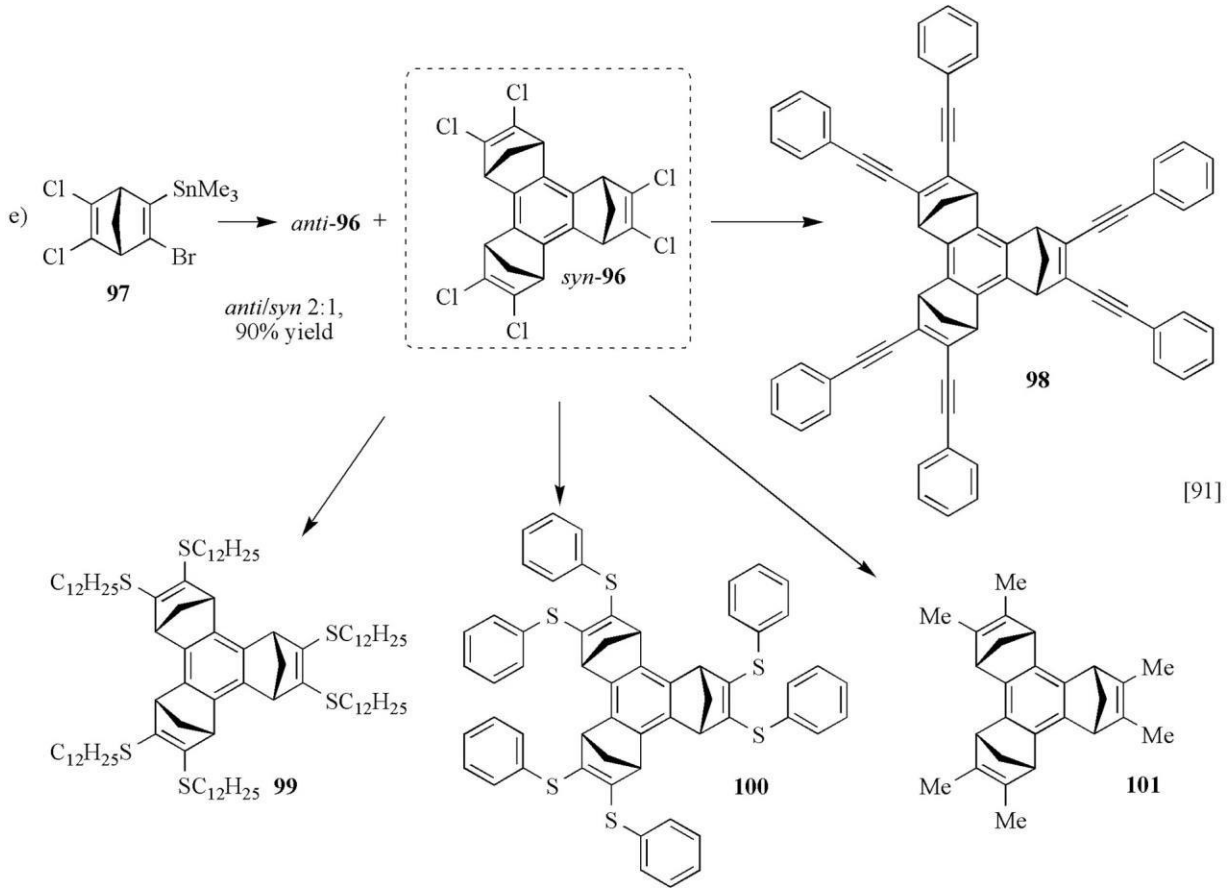

498498

499 **Scheme 14.** CuTC-mediated cyclotrimerization of polycyclic alkenes affording BTCs and related derivatives (*continued*).

500 The hexaester **91** was then converted to a stable tris-anhydride **92**, which, in a reaction with amines
501 followed by subsequent hydrogenolysis, yielded **93**, **94**, and **95**, in 76, 61, and 10% yield, respectively
502 (Scheme 14d). In 2005, Lucchini, Borsato *et al*. obtained well-defined and rigid molecular domes
503 (Scheme 14e) [91] by substitution of the chlorine atoms of hexachlorotrinorbornadiene *syn*-**96** which
504 was synthesized in 1 : 2 *syn*/*anti* ratio by CuTC-promoted cyclotrimerization of alkene **97**. The three
505 dichlorovinyl functionalities at the edge of *syn*-**96** were displaced by sulfur nucleophiles and Grignard
506 reagents with Ni(II)Cl_2dppe as catalyst, affording BCTs **98**-**101**. Starting from BCT **96**, the authors also
507 synthesized hexacarboxytrindanes in high yields through oxidative cleavage of the three double bonds of
508 the norbornene arms using $RuCl_3 \cdot 3H_2O/NaIO_4$ [92].

509 BCTs featured by heteroatoms, such as oxygen and nitrogen atoms, located at the apical positions of
510 bridged systems were also synthesized (Scheme 15). Balci, Fabris *et al*. developed an efficient synthetic

access to concave-shaped molecules by preparing potentially ionophoric *syn*- and *anti*-isomers of 5,6,11,12,17,18-hexahydro-5,18:6,11:12,17-triepoxytrinaphthylene (**102**) by CuTC-mediated cyclotrimerization of **103** (Scheme 15a) [93]. The BCT **102** was obtained in a *syn*/*anti* ratio of 5 : 4. In 2005, Zonta *et al*. performed the cyclotrimerization reaction of *N*-tosyl protected alkene **104** using CuTC at -20 °C for 1 h (Scheme 15b) [94]. The reaction afforded the *N*-tosyl (Ts) protected BCTs *anti*- and *syn*-**105** in 82% yield in 1.2 : 1 ratio. Again using *N*-Ts protected starting material, the authors also performed the synthesis of BCT **106** by using alkene **107** as starting material. In this case, BCTs *syn*- and *anti*-**106** were obtained in a 1:3 statistical ratio (Scheme 15c) [94].

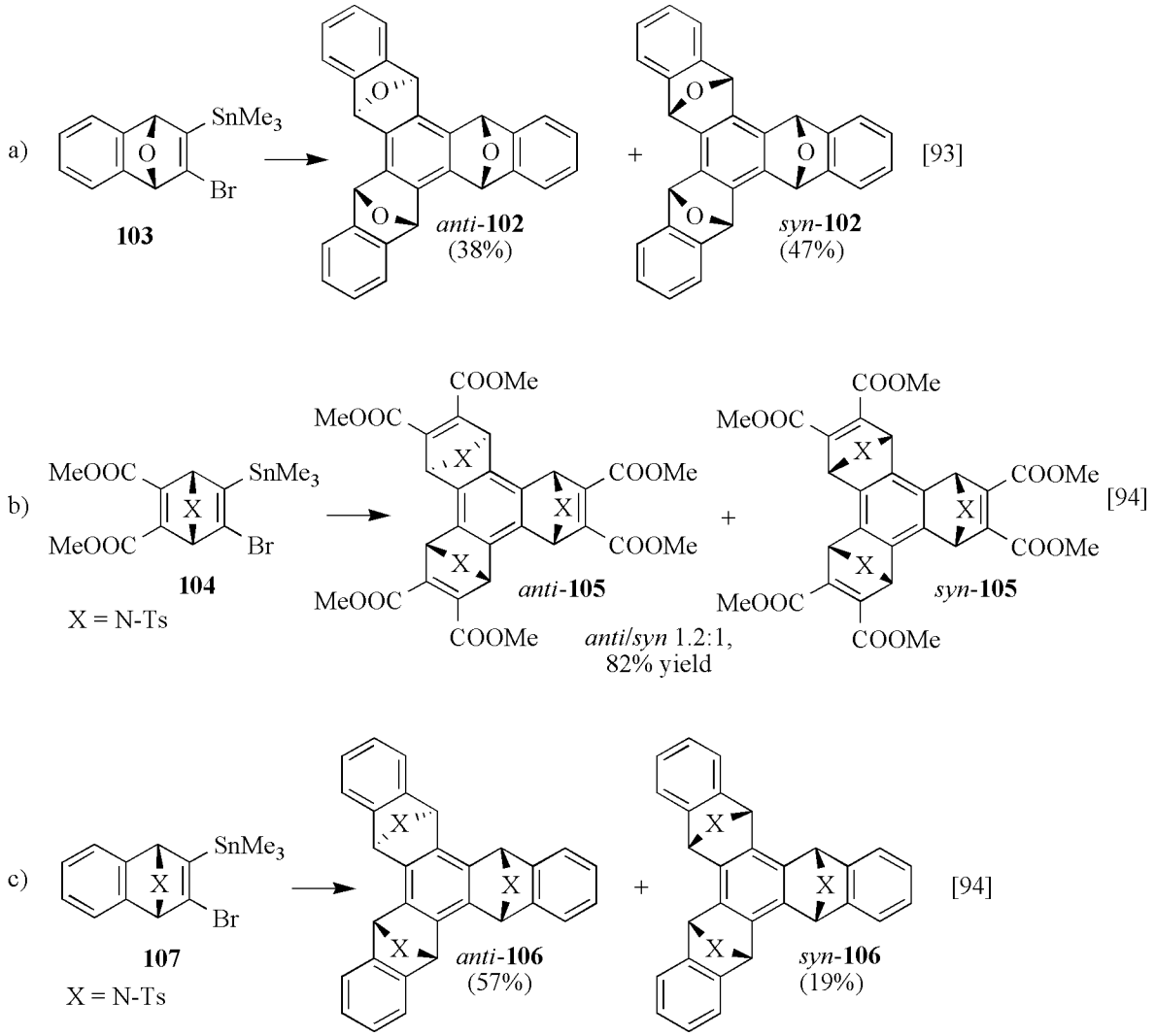

Scheme 15. CuTC-mediated cyclotrimerization of polycyclic alkenes affording BTCs functionalized at the apical positions.

Interestingly, the ^{1}H NMR spectrum for compound *anti*-**106** showed unexpected high field chemical shifts of the protons of a tosyl group at the apical position. Indeed, in this compound, the pocket formed by the two contiguous aromatic rings generated a cleft in which the electron-poor tosyl group forms a double edge-to-face interaction.

4.2.2 Synthesis of bridged BCTs through palladium-catalyzed cyclotrimerization

The first procedure to perform cyclotrimerization of polycyclic alkenes using a palladium catalyst was developed by Kochi *et al*. in 1998 [95]. This synthetic methodology of tris-annelated benzenes was based on the direct cyclotrimerization of a 1,2-dibromoalkene with 2 equiv of a vinylic Grignard reagent through the following steps: *a*) the coupling of the (1:2) components with a palladium catalyst to afford a linear 1,3,5-triene, *b*) *in situ* spontaneous sigmatropic rearrangement to the a dihydrobenzene, *c*) aromatization to the final BCT. By using bis(triphenylphosphine)palladium(II) as a catalyst, both symmetrical and unsymmetrical BCTs were obtained in high yields ranging from 84 to 97%. The *syn*/*anti* stereoselectivity was found to be dependent on the structure of the olefinic reagent, being 1 : 3 for BCT **26**. The 2,3-dibromobicyclooctene (**108**) and the corresponding Grignard reagent **109** afforded the tris-bicyclo[2.2.2]octanobenzene **34** in 97% yield.

In 2000, De Lucchi *et al*. described a method of preparation of BCTs which is based on the Stille coupling reaction [96, 97]. When bromotrimethylstannyl alkene **60** was heated at 70 °C for 24 h in DMF in the presence of palladium(II)acetate (10% mol eq.), triphenylphosphine (20% mol eq.) and LiCl, a 1 : 4 *syn*/*anti* mixture of BCT **46** was obtained in 38% yield. Under these experimental conditions, no detectable formation of dimers was observed, whereas dimers had been identified by the same authors in the reaction with copper nitrate [52]. Under palladium catalysis, yields and *anti*/*syn* ratio were found to be affected by temperature, solvent or by the changes to the other reaction conditions. For instance, the same reaction carried out in toluene at 120 °C afforded, after 24 h, 1 : 3 *syn*/*anti* mixture of BCT **46** in 30% yield. Otherwise, in refluxing THF, the system resulted unreactive even after 94 h. While the effect of co-catalysts such as LiCl did not significally improve the yields of the reaction, the bromotributyltin

benzonorbornadiene **110** treated with $Pd(OAc)_2$ (7% mol eq.) and PPh_3 (14% mol eq.) at 110 °C for 24 h in toluene led to BCT **46** as *anti* isomer in 58% yield. Evaluating the toxic nature of tin compounds, De Lucchi's group also tested the feasibility of the *in situ* formation of the tin starting material, under the conditions developed by Grigg [98]. Thus, by heating a mixture of dibromobenzonorbornadiene **47**, $Pd(OAc)_2$ (10% mol eq.), PPh_3 (20% mol eq.) and hexamethylditin in refluxing toluene, only BCT *anti*-**46** was obtained in 50% yield. Using hexabutylditin instead of hexamethylditin, the reaction afforded BCT **46** in quantitative yield. Through this optimized Grigg variant, also BCTs *anti*-**26**, **34**, and *anti*-**64** were obtained in high yields [97].

Later, Cossu, De Lucchi *et al*. carried out the cyclotrimerization of the bromobenzonorbornadiene **61**, under the condition of the Heck reaction [99, 100], by treating the starting alkene with $Pd(OAc)_2$ (5% mol eq.), PPh_3 (10% mol eq.), Et_3N (2.5 mol eq.), and *n*-Bu_4NBr (1 mol eq.). The reaction afforded *anti*-**46** in 95% yield (Scheme 16a). Under these conditions, the *anti*-isomers of BCTs **26**, and **62**-**64** were obtained in 90-95% yields. The authors noticed no formation of dimers in the course of the reaction. The tetraalkylammonium salts showed to have a pivotal role in the cyclotrimerization because the reaction carried out in the presence of *n*-Bu_4NHSO_4, as well as *n*-Bu_4NCl, or *n*-Bu_4NBr, reached completion within 48 h, whereas it proceeded very slowly without added ammonium salts (7 days, 80°C, 70% conversion) [99]. As shown in Scheme 16b, the formation of complex **113** was hypothesized to occur through base-induced E_2 elimination of HBr at the stage of the σ-complex **112**. Complex **113** may carbopalladate another molecule of bromoalkene to afford the cyclic trimer **114**, which undergoes 6π electrocyclization to the cyclic trimer **115**, and subsequently elimination, as in the standard Heck reaction. The origin of the stereoselectivity affording to the exclusive formation of the *anti*-isomer could be attributed to the steric overcrowding in homochiral dimeric Pd-complex (Scheme 16c, left) which is disfauvored compared to the heterochiral dimeric Pd-complex (Scheme 16c, right) [99]. As confirmation, the reaction performed by using the enantiopure **61** was shown to proceed much more slowly than that carried out with the racemate, affording a mixture of *syn*- and *anti*-BCTs **46** in ca. 3 : 1

ratio, together with substantial amounts of unidentified products. Under the Heck-reaction conditions, *rac*-2-iodobenzonorbornadiene afforded *anti*-**46** in comparable yields. Otherwise, in the cyclotrimerization of (1*R*)-2-iodobornene under Heck conditions, Fabris *et al*. obtained a mixture containing *syn*- (5% yield) and *anti*-BCT (2% yield), along with dimerization (52% yield) and benzocyclodimerization (25% yield) products [101].

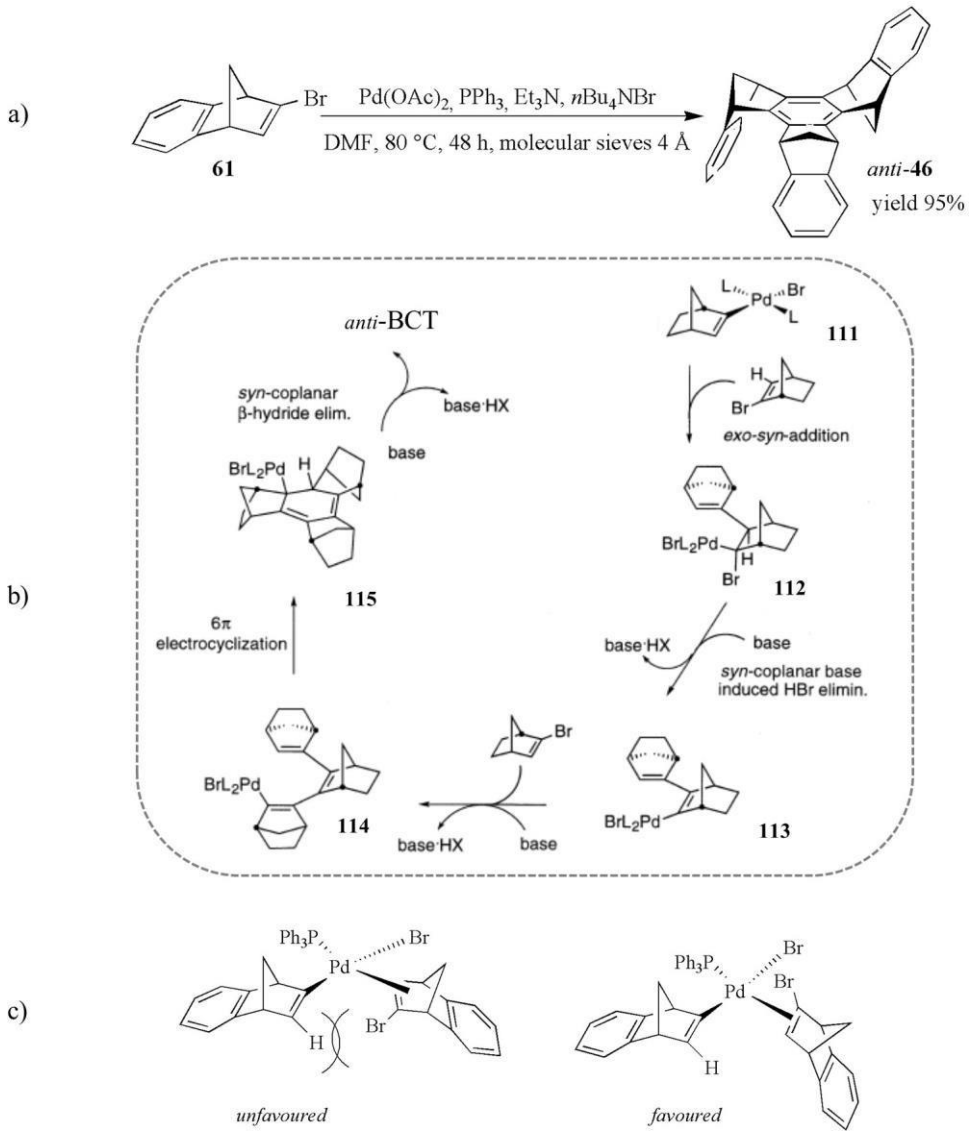

Scheme 16. *anti*-Selective Heck-type cyclotrimerization of a) 2-bromobenzonorbornadiene **61**, b) mechanism of cyclotrimerization, and c) structures of diastereomeric Pd-complexes (adapted with permission from ref. 99).

In 2007, Sakurai and co-authors reported the Pd-catalyzed cyclotrimerization of enantiopure iodonorbornenes to prepare C_3 symmetric enantiopure *syn*-tris(norborneno)benzenes under Pd-

582 nanocluster conditions [38]. The cyclotrimerization of iodobornene **116** under the Heck-reaction
583 conditions reported by Cossu and De Lucchi [99] did not take place, giving a complex mixture with only
584 a trace amount of *syn*-**117** (Table 3, entry 1).

585 **Table 3.** Palladium-catalyzed cyclotrimerizationof the enantiopure iodoalkene **116**.

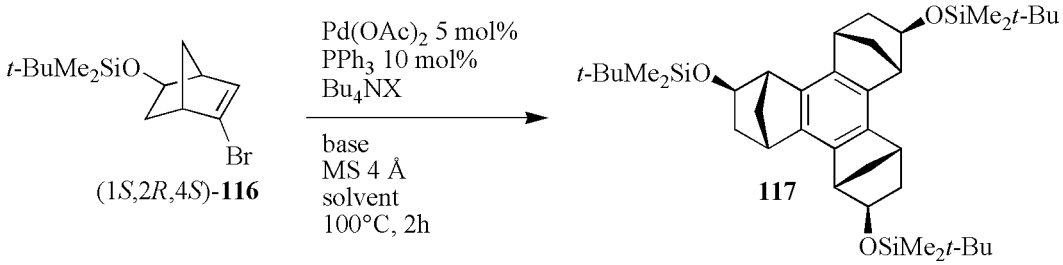

586586

Entry	Bu_4NX (mol%)		Base (mol%)		Solvent	%Yield of **117**
1[a]	Bu_4NBr	100	NEt_3	250	DMF	trace
2	Bu_4NOAc	100	Na_2CO_3	1000	1,4-dioxane	34
3	Bu_4NOAc	300	Na_2CO_3	1000	1,4-dioxane	42
4	Bu_4NOAc	500	Na_2CO_3	1000	1,4-dioxane	47
5	Bu_4NOAc	1000	Na_2CO_3	1000	1,4-dioxane	53

587 [a] Conditions reported in ref. [99].

588 After screening several conditions, Sakurai *et al*. found that *syn*-**117** could be obtained in 34% yield
589 as a single isomer by using Bu_4NOAc and Na_2CO_3 in 1,4-dioxane solution (Table 3, entry 2). In
590 particular, the yield of BCT **117** was dependent on the amount of Bu_4NOAc, indicating that the Pd
591 nanoclusters generated in the reaction mixture may play an important role. On this basis, the yield was
592 improved to 53% by increasing the amount of Bu_4NOAc to 1000 mol% (Table 3, entries 2–5).
593 Interestingly, the authors reported photographs and typical TEM images of the reaction mixtures under
594 the conditions listed in entries 1, 2, 4, and 5 in Table 3 (Fig. 13). The Pd nanoclusters were shown to be
595 well dispersed in the order of (B) < (C) < (D) which was consistent with the amount of Bu_4NOAc. The
596 amount of precipitation of Pd black was observed in the opposite order, (B) > (C) > (D). Moreover, the
597 appearance of (A) was similar to that of (D), indicating the formation of nanoclusters. However, a
598 considerable degree of aggregation of clusters was observed in the TEM image (A) as well as in the
599 image (B). These observations strongly suggested that the generation of Pd nanoclusters in appropriate

conditions might be very important, and that using an excess amount of Bu_4NOAc could realize well-dispersed nanoclusters.

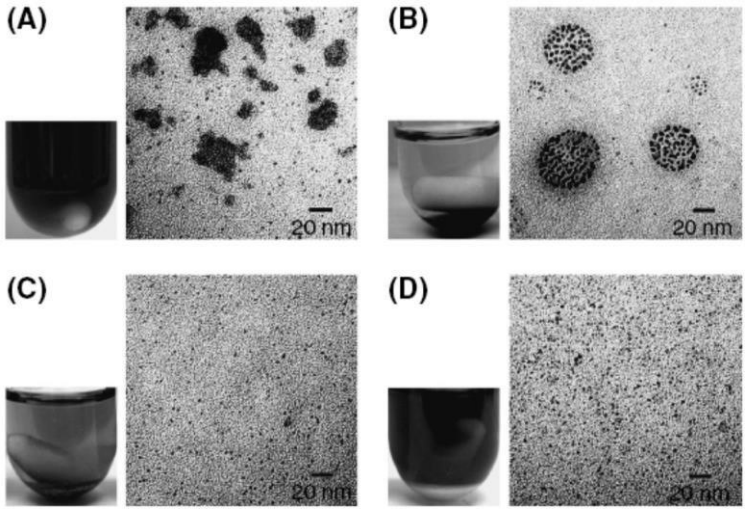

Fig. 13. Photographs and typical TEM images of Pd-nanocluster-catalyzed reaction mixtures (Table 3): (A) entry 1, (B) entry 2, (C) entry 4, and (D) entry 5 (reproduced with permission from ref. 74).

The authors noticed that role of the Pd nanoclusters in the process may be understood in relation to the mechanistic insight of the Heck reaction. Indeed, *a*) given that for the Heck reaction atomic palladiums leached from nanoclusters were reported to be the active species, and *b*) since there are two Heck-type insertion steps at sterically hindered positions (see Scheme 16b), the Pd-nanocluster catalyzed reaction was reasonably believed to be controlled by the active Pd species continuously leached from the high concentrated Pd nanoclusters [38]. Exploiting this procedure, Sakurai's group prepared a series of C_3-symmetric homochiral *syn*-tris(norbornabenzene)s through the regioselective cyclotrimerization of enantiopure iodonorbornenes [74]. In particular, the authors performed the cyclotrimerization of chiral iodonorbornene derivative (1*S*,4*S*)-**118** to afford *syn*-benzocyclotrimer **119** without contamination of the diastereomer *anti*-**119** (Scheme 17) [102]. The carbonyl groups of **119** could be converted to methyl-substituted BCT **120** through alkenyl phosphates by cross-coupling reactions with MeMgI. Treatment of **120** with Grubbs first generation catalyst afforded a mixture of only ROM products. Otherwise, Grubbs second generation catalyst was effective for the RCM, giving **121**. The final aromatization step was

carried out with 2,3-dichloro-5,6-dicyano-*p*-benzoquinone, obtaining the chiral buckybowl (*C*)-(*M*)-8,13,18-trimethylsumanene (**122**).

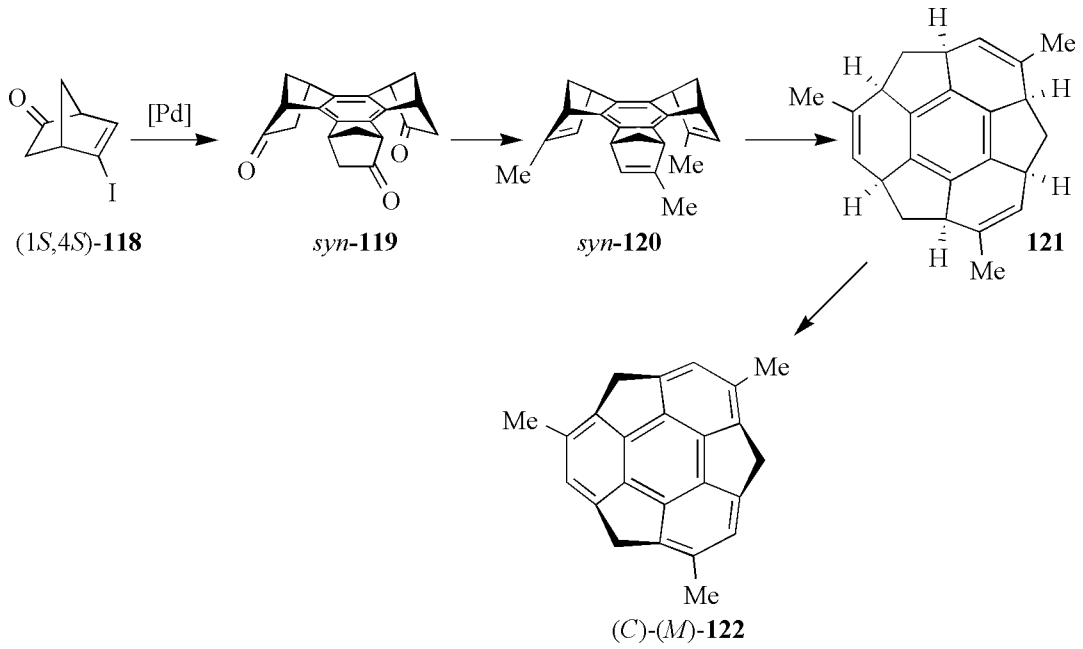

Scheme 17. Synthesis of (*C*)-(*M*)-8,13,18-trimethylsumanene (**122**) starting from enantiopure polycyclic iodoalkene **118**.

This strategy has allowed the authors to access several C_{3v} and chiral C_3 BCTs [74, 103]. They noticed that observed *syn*/*anti* selectivity caused by substituents ranged from 100 : 0 to 77 : 23. As a general trend, higher *syn*-selectivity was observed for C_3 symmetric tris(norborneno)benzenes than C_{3v} symmetric ones [104]. On this basis, over time, Sakurai's group have prepared and studied sumanenes characterized by different types of functionalization [103,105,106]. The group also elucidated the reaction mechanism as well as the stereoselectivity of the Pd-catalyzed cyclotrimerization through DFT calculations [107], confirming that the reaction pathway consists of *a*) sequential olefin insertion followed by an HX elimination reaction of halonorbornene with the norbornenylpalladium intermediate, *b*) electrocyclization of the trienylpalladium intermediate with a lower activation barrier than a triene compound, and *c*) the β-elimination of HPdX of the cyclohexadienylpalladium intermediate. In addition, the stereoselectivity would be controlled by the regioselectivity in the olefin insertion process (homo and hetero positions) and the symmetry breaking in the palladacyclic intermediate.

634 It is worth mentioning that very recently, Badjić subjected to cyclotrimerization the enantiopure
635 dimethyl (1*S*,4*S*)-2-iodo-1,4-dihydro-1,4-methanonaphthalene-6,7-dicarboxylate (**123**) under the Pd-
636 nanocluster catalyzed conditions described by Sakurai, recovering the unreacted starting material
637 exclusively [80]. This result showed that also under Pd-nanocluster catalysis the cyclotrimerization tends
638 to be dependent on the structure of the starting polycyclic alkene. Later, Badjić's group obtained
639 moderate yield of three new BCTs having increasingly deeper and extendable aromatic cavities with
640 high *syn*-stereoselectivity by using Pd-catalysis with neocuproine (DMPHEN) as a bidentate nitrogen
641 ligand and 4-(dimethylamino)pyridine (DMAP) to displace the ligand in the migratory insertion, which
642 is a key step of the cyclotrimerization [39]. In 2008, the same group had also investigated the
643 supramolecular assistance to double Pd(0)/Cu(I)-catalyzed cyclotrimerization of stannylated norbornene
644 **124** to give the molecular bowl *syn*-**125** in a stereoselective fashion (Scheme 18) [108].

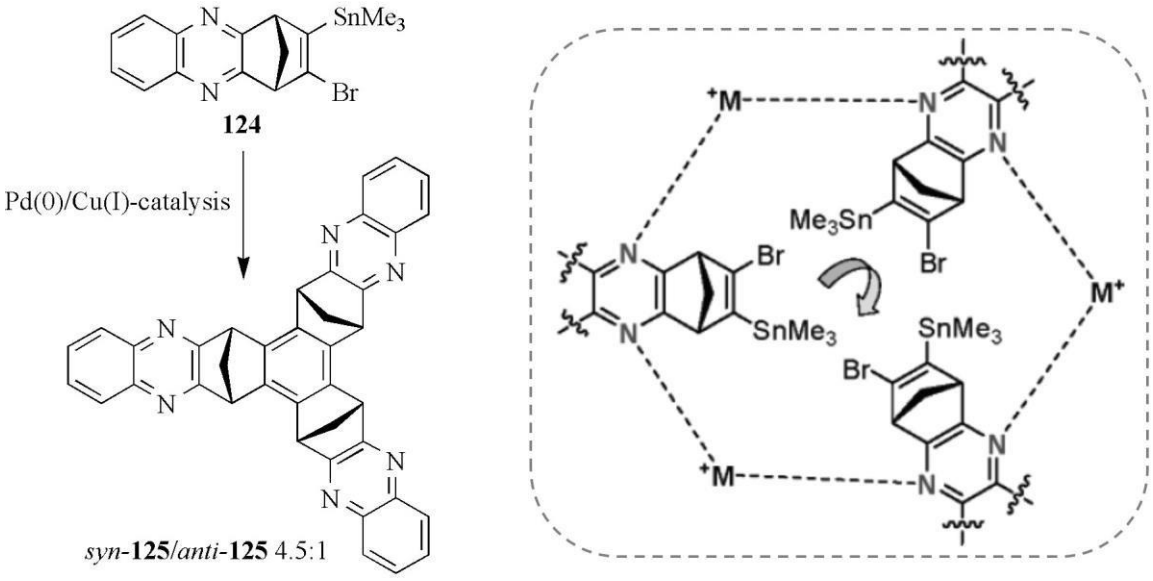

645645

646 **Scheme 18.** Supramolecular assistance in Pd(0)/Cu(I)-catalyzed cyclotrimerization (adapted with permission from ref.
647 108).

648 The self-coupling of *rac*-**124** was found to be promoted by Pd(0)/Cu(I) catalysis acting in synergy
649 with CsF, providing *syn*-**125** in a moderate 30% yield. The reaction diastereoselectivity resulted to be

affected by the concentration of Cu(I) and Cs^+, increasing quantities of the cations enhancing the *syn*/*anti* ratio of the isolated cyclotrimer from statistical 1 : 3 to the more attractive 4.5 : 1 ratio.

5. BRIDGED BCTs AS CONCAVE SYNTHETIC RECEPTORS

The first observations that bridged BCTs showed a strong ability to complex solvent molecules in their arene-lined cavities date back to the 1990s. For instance, Bürgi, Siegel *et al*. obtained crystalline **20** in the form of a 1:1 complex with chlorobenzene, in which the solvent molecules packed in channels between ribbons of molecules of the BCT [67]. The crystal packing was shown to distort the molecular structure of **20** away from the idealized D_{3h} form expected for the isolated molecule. Later, Kochi *et al*. studied the molecular association of **26** and **34** as aromatic π-donors with diverse π-acceptors by X-ray diffraction, spectroscopy and computational analyses [109], observing that some acceptors could approach the BCTs despite the steric hindrance exerted by these structures.

It was in the late 1980s that Stoddart *et al*. synthesized trinacrene (**125**) as the first cage based on a bridged BCT structure (Scheme 19) [35, 110]. Compound **125** was synthesized in four steps starting from hexabromobenzene (**126**) and furan (**127**), through the formation of BCT *syn*-**53**, but in a low overall yield < 0.01% [110-112].

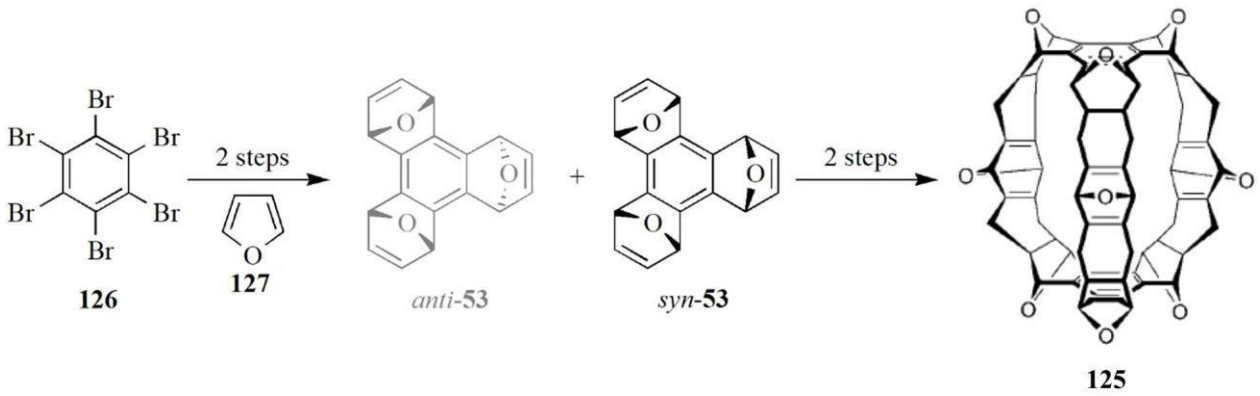

Scheme 19. Synthesis of trinacrene (**125**) (adapted with permission from ref. 111).

In 2000, in light of Klärner's findings [113], De Lucchi *et al*. investigated the electronic structures of the BCTs *syn*-**46**, and *syn*-**62**-**64** by calculating the electrostatic potential surfaces (EPSs) of these molecules [76]. On this basis, it was found that the concave sides of the BCTs exhibit highly negative

electrostatic potential (EP) values, while, on the outer surface, the values are comparable with those of polyalkylated benzenes (Fig. 14a). This evidence suggested high complexing capability with molecules bearing electron-poor regions with postive EP values. Moreover, *syn*-**46** showed to be able to draw fullerene C_{60} into acetonitrile solution, a solvent unable to solubilise fullerenes. Indeed, given that UV absorption of C_{60} in acetonitrile is completely absent because of its insolubility, and pure *syn*-**46** also does not absorb in this region, the comparison of the UV spectrum of *syn*-**46**, and that of an acetonitrile solution of *syn*-**46** after addition of C_{60}, might be considered as a proof of *syn*-**46**/C_{60} complex formation (Fig.14b).

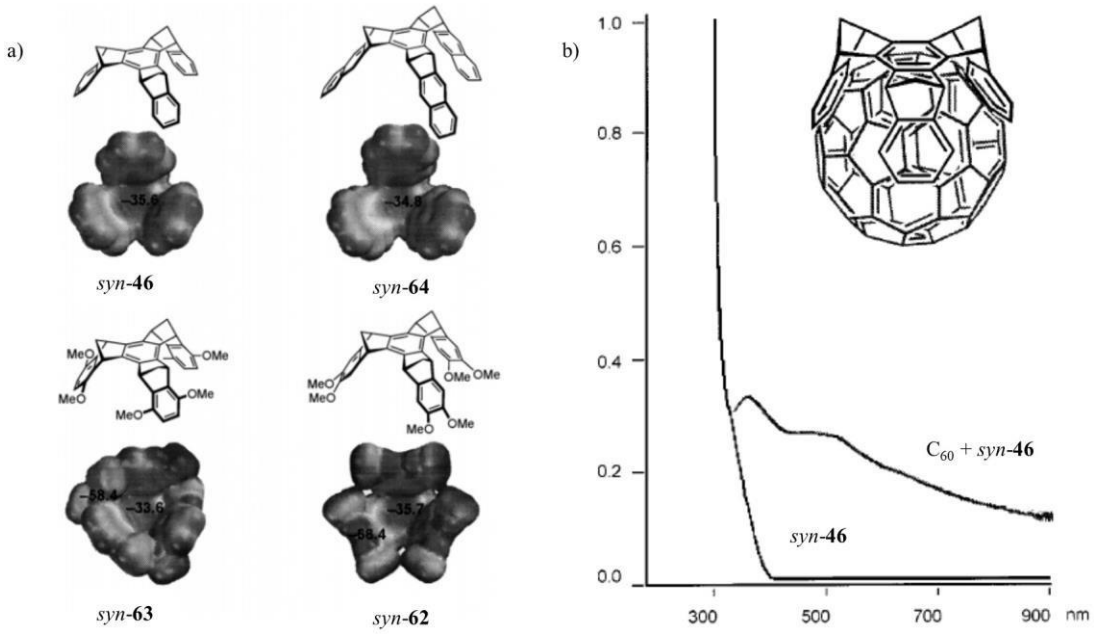

Fig. 14. a) EPSs of BCTs *syn*-**46**, and *syn*-**62**-**64** calculated at semiempirical AM1 level, and b) UV spectra of an acetonitrile solution of *syn*-**46** (10^{-3} M) and of the same solution after addition of C_{60} (excess) (adapted with permission from ref. 76).

Starting from the early 2000s, inspiring to the conformational rapid opening and closing of the gate to the active site of enzymes [114], Badjić and co-authors have developed a research program which is oriented to design, synthesize and study molecular baskets and cavitands with allosterically controllable conformational dynamics to allow for the regulation of molecular recognition and reactivity [40, 90, 115].

686 The first baskets prepared by the group were BCTs **93-95** containing three phenolic gates (Scheme
687 14d) [90]. However, these baskets were incapable to retain guests due to a poor pre-organization of the
688 cavities, and limited solubility in solvents incapable of occupying their cavities [40]. Later, with the
689 assistance of computational chemistry, a series of BCTs of general structure **128**, bearing amido-
690 pyridine gates, was designed, synthesized and successfully used as molecular baskets for encapsulation
691 and dynamic discrimination of small molecules in the enclosed space (Fig. 15) [40, 115-123]. This
692 pyridine-based gates are each conjugated to the framework via a CH_2 as a rotor, and also decorated with
693 an amide functional group. The amide groups were found to adopt a *Z* configuration about each C-N
694 bond with the basket's pyridine gates forming three intramoleuclar N-H···N hydrogen bonds (HBs)
695 [117].

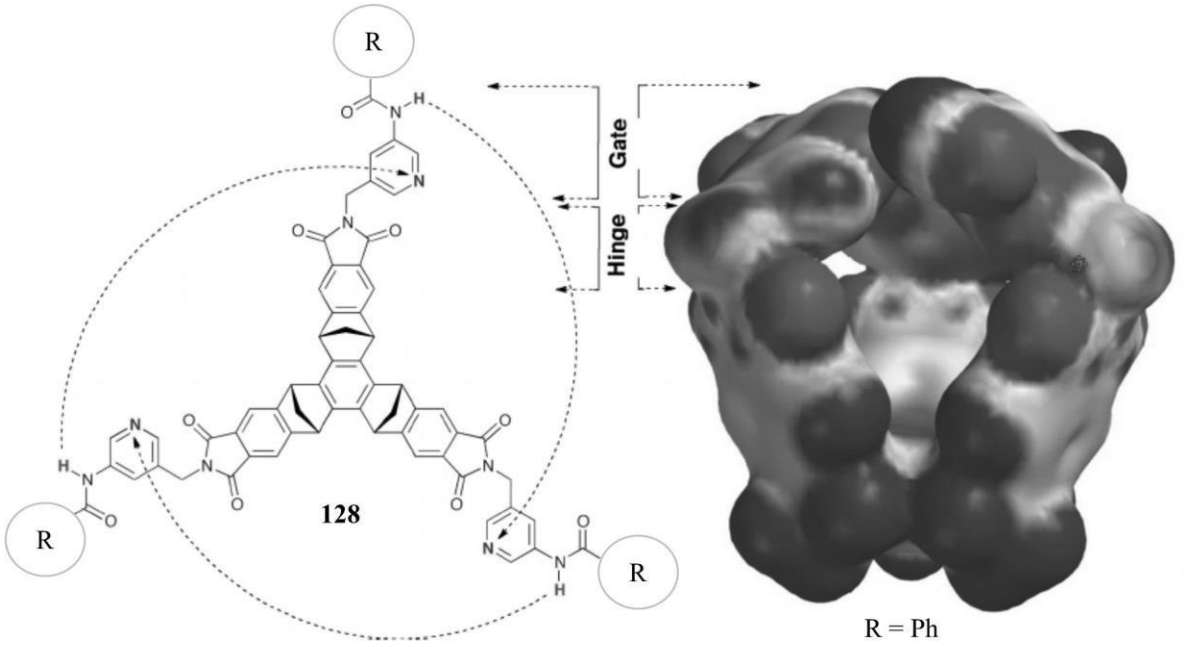

696

697 **Fig. 15.** General structure of amido-pyridine molecular baskets **128**, and electrostatic potential surface of basket **128** with
698 R = Ph (adapted with permission from ref. 123).

699 A series of studies performed by Badjić's group concerns the use of a transition metal to enclose
700 space by bringing together ligands appended to a tridentate bowl-shaped host, thus allowing the
701 coordinatively unsaturated metal to further bind another molecule by placing it inside or outside the

cavity [124]. The authors hypothesized that the encapsulation and detection of target molecules in such hosts could be greatly facilitated by means of coordination, allowing chemical reactivity in dynamic and confined environments to be modulated. On this basis, the properties of BCTs *syn*-**129**-**133** as tridentate compounds, containing three pyridine flaps tethered to a semirigid scaffold, were explored through experimental and theoretical methods (Fig. 16) [124-126]. The Ag(I) mediated folding of *syn*-**130** into a molecular basket was shown to be highly favorable in organic media, with the assembly process allowing for another ligand to bind preferentially on the outer side [124]. DFT calculations of the optimized geometries of the folded basket showed that the three pyridine moieties, coordinated to Ag(I), are twisted in the same direction with a propeller-like geometry, and with either a *P* or *M* sense of twist.

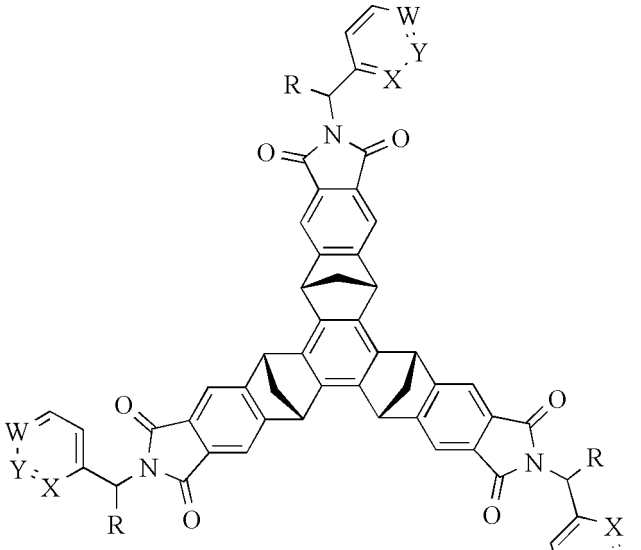

129, X = N, Y = H, W = H, R = H
130, X = H, Y = N, W = H, R = H
131, X = H, Y = H, W = N, R = H
132, X = H, Y = H, W = H, R = H
(*S*)-**133**, X = H, Y = N, W = H, R = Me
(*R*)-**133**, X = H, Y = N, W = H, R = Me

Fig. 16. Structures of molecular baskets **129**-**133**.

BCT *syn*-**130** also showed to coordinate to a Cu(I) cation, and thus folded in a multivalent fashion [125]. Variable temperature ^{1}H NMR, 2D COSY, and ROESY investigations revealed the existence of a first Cu(I)-folded basket with a molecule of acetonitrile occupying its interior and coordinated to the metal. Interestingly, the basket was shown to be in equilibrium with a second Cu(I)-folded form, whose

717 inner space is solvated by acetone or chloroform used in the NMR experiments. The conversion between
718 the two forms was shown to necessitate a molecule of acetonitrile to displace the solvent in the cavity of
719 the second Cu(I)-folded form. The addition of neat acetonitrile to a solution containing both forms of the
720 Cu(I)-folded basket shifted the equilibrium toward the greater formation of the form including
721 acetonitrile. The behaviour of molecular baskets **129**-**132** was compared in terms of Ag(I) coordination
722 [126]. For BCTs **130** and **131**, the position of the nitrogen was revealed to have an effect on directing the
723 basket's coordination to Ag(I) cation, and subsequent folding to enclose space. Moreover, CH_3CN was
724 not found inside of the basket Ag(I):**130**, this evidence being in contrast with the behavior of Cu(I):**130**
725 [125]. The X-ray solid-state structural studies of **129**, **130**, and **131** revealed the capability of the baskets
726 to fill their inner space with small compounds. Thus, **130** was found with an ordered molecule of
727 chloroform, while **131** contained molecules of CH_3OH and H_2O. Later, Badjić's group extended the
728 investigation to chiral molecular baskets (R_3/S_3)-**133** containing three pyridine rings at the rim of a bowl-
729 shaped platform, each pyridine being tethered to the platform via a $CH(CH)_3$ stereogenic center [127].
730 According to the results described in the previous lines, the authors found that chiral basket (R_3)-**133**
731 coordinates to Ag(I) cation, and that the $CH(CH)_3$ stereogenic center may direct the twisting of the
732 pyridine rings at the rim in a clockwise orientation (*P* configuration). Thus, the results of both
733 experimental and computational investigations suggested that a stereogenic alkyl center at the "hinge"
734 position may control dynamic stereoisomerism in basket-like systems through chirality transfer in Ag(I)-
735 folded basket structure. In 2016, the same group examined the structural and electronic
736 complementarities of convex **134**−Zn(II), comprising functionalized tris(2-pyridylmethyl)amine (TPA)
737 (**135**) ligand, and the concave baskets **136** and **137**, having glycine and (*S*)-alanine amino acids at the
738 rim, respectively (Fig. 17) [128]. With the assistance of ^{1}H NMR spectroscopy and mass spectrometry,
739 they found that basket **136** entraps **134**−Zn(II) in water to give equimolar **134**−Zn⊂**136**$_{in}$ complex,
740 resembling Russian nesting dolls. Again, the enantiopure basket **137**, containing (*S*)-alanine groups at
741 the rim, was found to transfer its static chirality to entrapped **134**−Zn(II) and, *via* intermolecular ionic

742 contacts, twist the ligand's pyridine rings into a left-handed (*M*) propeller. Later, the performances of
743 both positively and negatively charged molecular baskets to form nesting complexes were comparatively
744 evaluated, observing that the primary driving force behind the formation of nesting complexes, from
745 complementary host/guest components, is the hydrophobic effect [129].

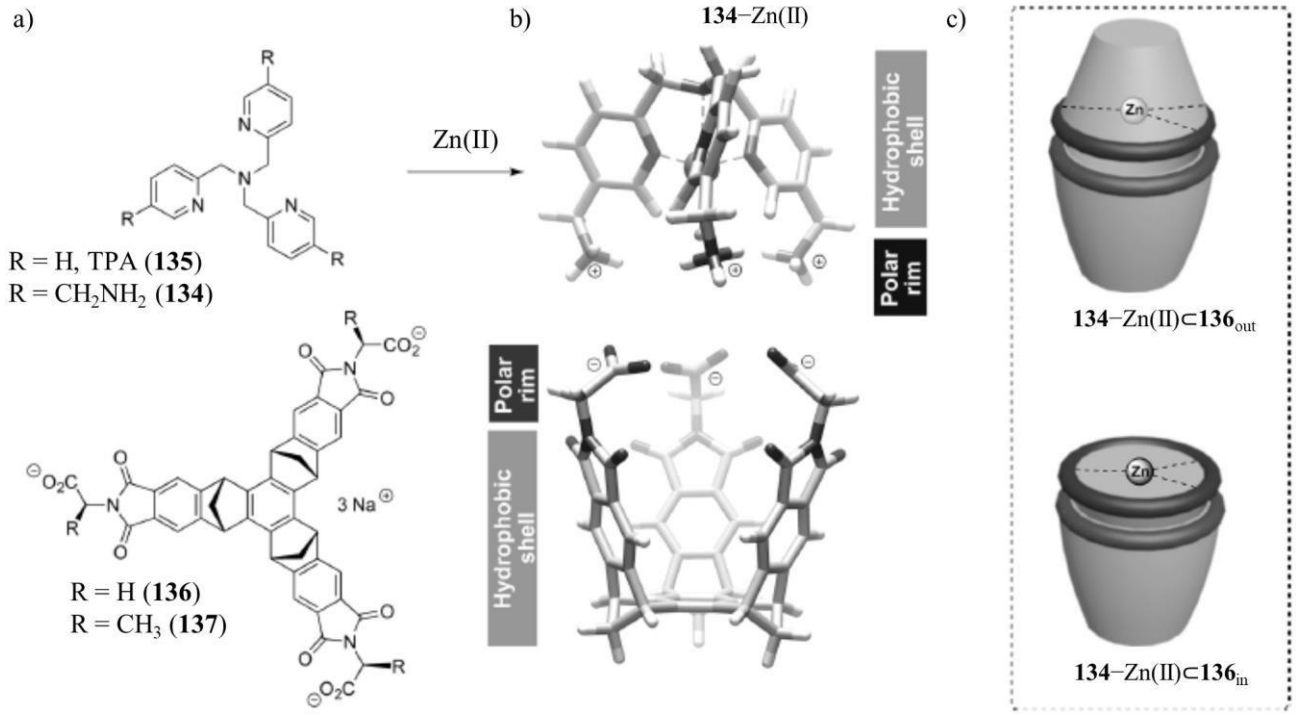

746746

747 **Fig. 17.** a) Chemical structures of tris(2-pyridylmethyl)amine (TPA) (**135**), derivative **134**, and molecular baskets **136** and
748 **137**, b) energy-minimized structures (MMFFs, Spartan) of C_3 symmetric **134**–Zn(II) and **136**, showing their electronic and 749
structural complementarity, and c) a schematic representation of two possible ways for the assembly of **134**–Zn(II)⊂**136** in
750 water, capsular **134**–Zn(II)⊂**136**$_{out}$ (top) and nesting **134**–Zn(II)⊂**136**$_{in}$ (bottom) (adapted with permission from ref. 128).

751 Recently, two molecular baskets, each containing three (*S*)-glutamic acids at its rim, were found to
752 complex diammonium alkanes, giving ternary assemblies [130]. The authors also found that molecular
753 baskets with amino acids at their rim, such as **136** and **137**, undergo photoinduced decarboxylation to
754 give the corresponding baskets with alkylated phthalimide terminations, forming a solid precipitate in
755 water [79]. Interestingly, organophosphonates, similar in size and shape to *G*-type nerve agents, form
756 inclusion complexes with the alkylated baskets, light irradiation (300 nm) of an aqueous solution of
757 these inclusion complexes leading to the formation of precipitate containing the organophosphonate

compound. In this field, Badjić's group also observed that an amphiphilic phthalimide basket is able to assembles into unilamellar vesicles in water [131]. The assembled host encapsulates organophosphonates, their entrapment prompting a phase transformation of the vesicular basket into nanoparticles or larger vesicles as a function of the shape of the host−guest complex. Recently, other photoresponsive materials able to transform molecular baskets into organic nanoparticles have been also explored by the group [132-134]. Other recent applications of bridged-featured molecular baskets developed by Badjic and co-authors can be grouped in the following classes:

a) *molecular capsules* – In 2018, the authors reported the preparation, conformational dynamics, and recognition characteristics of a novel molecular capsule **138** formed by a bowl-shaped framework conjugated to a tris(2-pyridylmethyl)amine (TPA) lid (Fig. 18a) [135]. By integrating ^{1}H NMR experiments and theorethical calculations (MM and DFT), C_3 symmetric **138** was found to be poorly preorganized with three pyridines at the rim adopting a propeller-like orientation and undergoing *P*-to-*M* (or *vice versa*) stereoisomerization ($\Delta G^{\ddagger} < 8$ kcal/mol). Capsule **138** was also shown to bind small molecules such as CH_4, CH_3Cl, CH_2Cl_2, $CHCl_3$, and CCl_4 with $K_a < 7$ M^{-1}. Protonation of **138** with HCl, however, gives [**138**·H]−Cl, with the solid-state structure showing the TPA lid being "flattened" and the $^{+}$N−H···Cl hydrogen bonded group residing outside. It was noted that the *P*-to-*M* stereoisomerization occurs for [**138**·H]−Cl with $\Delta G^{\ddagger} = 11$ kcal/mol. The less dynamic and more preorganized [**138**·H]−Cl basket was shown to bind CH_4, CH_3Cl, CH_2Cl_2, $CHCl_3$, and CCl_4 with a greater affinity (K_a = 100−400 M^{-1}) than **138**. Very recently, covalent capsule **139** was designed by the group to include two molecular baskets linked with three mobile pyridines tucked into its inner space (Fig. 18b) [41]. On the basis of both theoretical calculations (DFT) and experiments (NMR and X-ray crystallography), it was found that the pyridine "doors" split the chamber (380 Å^3) of **139**, so that two equally sizeable compartments (190 Å^3) became joined through a conformationally flexible aromatic barrier.

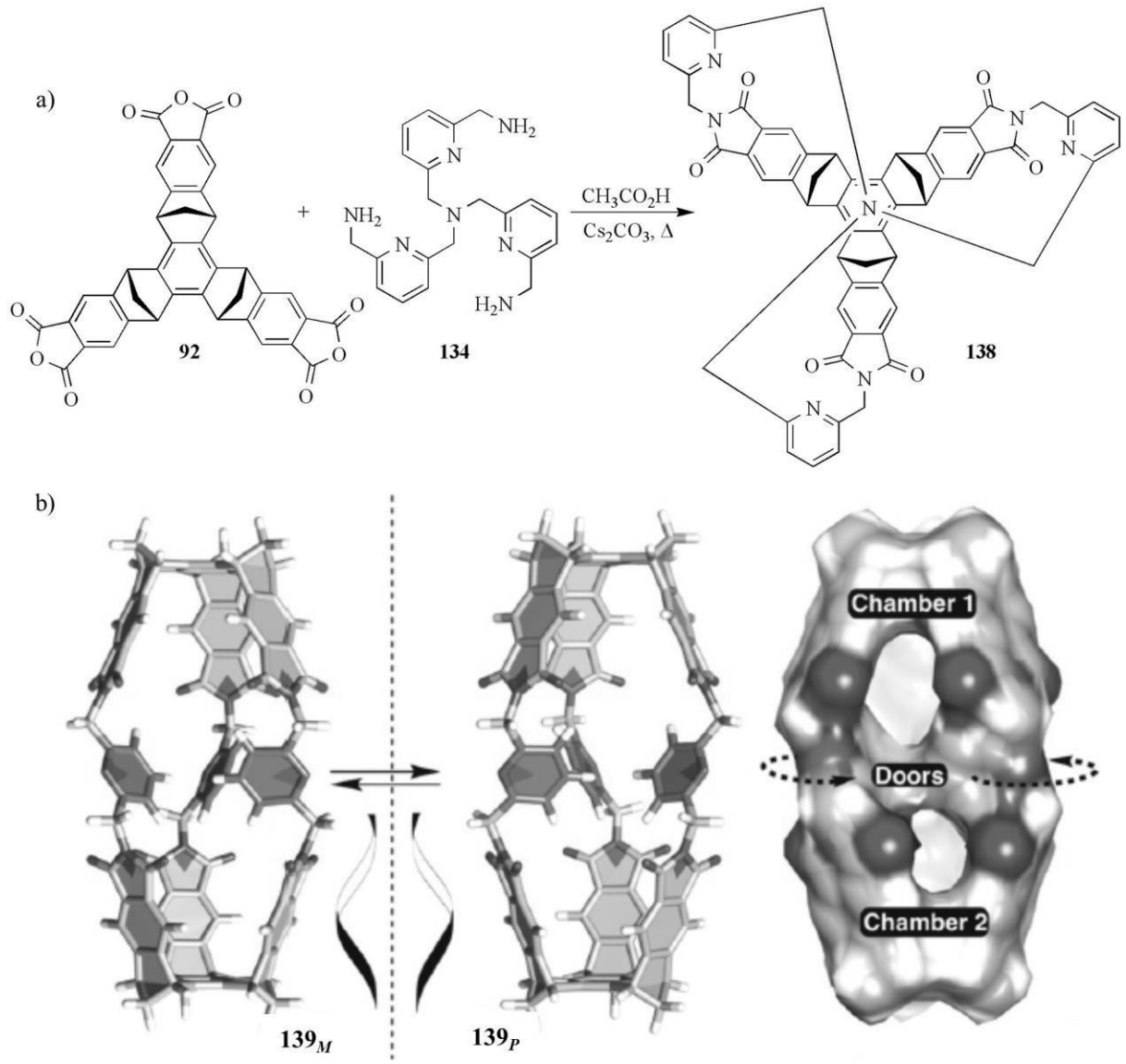

Fig. 18. a) Preparation of molecular capsule 138, and b) energy-minimized structures (DFT/M06-2X: 6-311++G**) of enantiomeric $\mathbf{139}_{M/P}$ capsules and their van der Waals surface (adapted with permission from ref. 41).

b) *baskets based on the bicyclo[3.2.1] platform* – Along with baskets featured by the bicyclo[2.2.1] motif, Badjić's group prepared and studied molecular basket **140** bearing amidopyridine gates, as in **128** (Fig. 15), but attached to a larger bicyclo[3.2.1] platform possessing either *P* or *M* chirality (Fig. 19) [136, 137]. In organic solvents, racemic (*P*/*M*)-**140** showed to form a sizeable C_3-symmetric capsule with a unidirectional seam of three N–H···N HBs. Later, chiral cavitands featured by the bicyclo[3.2.1] platform and bearing quinoline gates, at the rim of their twisted platform, were synthesized and studied [138]. These compounds showed to fold the quinoline gates in acetonitrile, giving molecular capsules

that assemble into large unilamellar vesicles. Otherwise, in the less polar dichloromethane, the cup-shaped compounds packed into vesicles but with the quinoline gates in an unfolded orientation. Finally, recently a capsule comprises a static, but twisted, bicyclo[3.2.1] cage that is linked to a dynamic tris(2-pyridylmethyl)amine (TPA) lid at its top was also explored by the group [139].

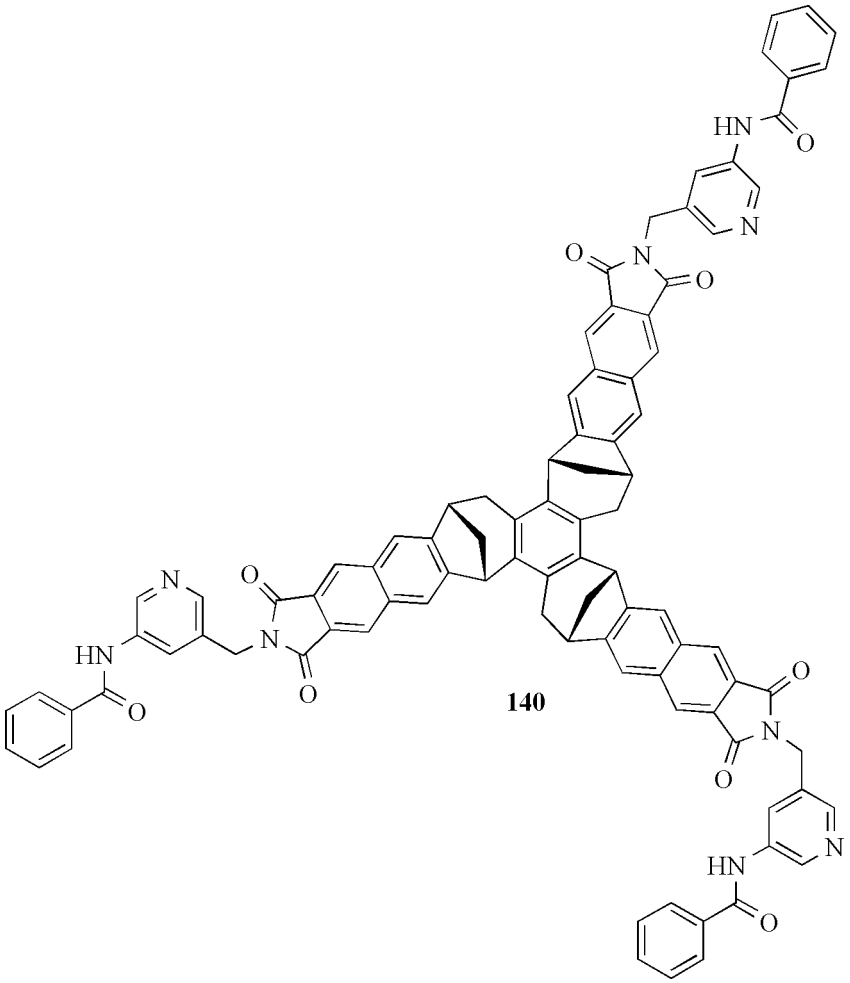

Fig. 19. Structure of bicyclo[3.2.1] cage **140**.

c) *dual cavity baskets* – In 2015, dual-cavity basket **141** was developed, which is characterized by six (*S*)-alanine residues at the entrance of its two juxtaposed cavities (289 Å^3) (Fig. 20) [140]. Through ^{1}H NMR spectroscopy and calorimetry, **141** was found to trap a single molecule of an adamantane derivative similar in size (241 Å^3) and polar characteristics to nerve agent VX (289 Å^3). Also in this case, integrating results of DFT calculations (M06-2X/6-31G*) and ^{1}H NMR experiments suggested that the negative homotropic allosterism arises from the guest forming C–H···π contacts with all three of the

aromatic walls of the occupied basket's cavity. In response, the other cavity increases its size and turns rigid to prevent the formation of the ternary complex, this dynamics being evaluated by comparing the values of the torsion angles χ_1 and χ_2.

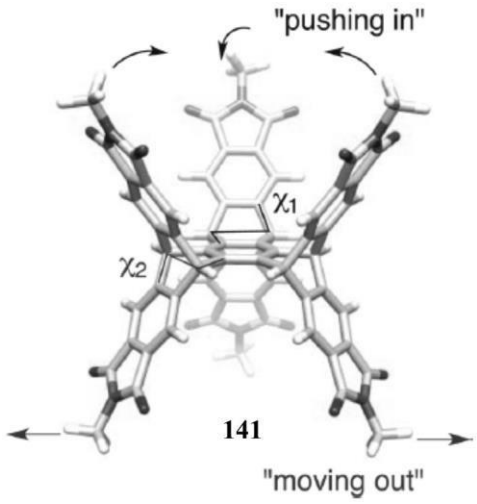

Fig. 20. Structure and dynamics of dual-cavity basket **141** (adapted with permission from ref. 140).

D$_3$ symmetric and chiral basket **142** (Fig. 21), containing six (*S*)-alanine residues at its termini, showed bolaamphiphilic properties as synthetic host [141]. This dual-cavity basket form large unilamellar vesicles [**142**]$_n$ in water by placing its hydrophobic framework inside the vesicular monolayer, while keeping six carboxylates at the interface with bulk water. Upon the addition of divalent paraquat **143** to [**142**]$_n$, the formation of equimolar [**142**−**143**]$_n$ resulted in the changing of the ζ-potential of the assembly. Thus, the guests were postulated to cover the vesicular surface, with each populating the inner space of two adjacent baskets thereby giving rise to a two-dimensional supramolecular polymer [142]. To test the encapsulation features of [**142**]$_n$, the authors treated it with a solution of rhodamine (RhB), as a biocompatible fluorophore, observing that a passive transport of cationic RhB molecules across negatively charged vesicular membrane of [**142**]$_n$ could be tuned with paraquat **143**. Indeed, this guest covering the curved surface of [**142**]$_n$, the resulting [**142**−**143**]$_n$ vesicles become impermeable to cationic RhB dyes. However, a conversion of the

complexed paraquat into its radical cation, forces the vesicular membrane to facilitate the passage of dye molecules.

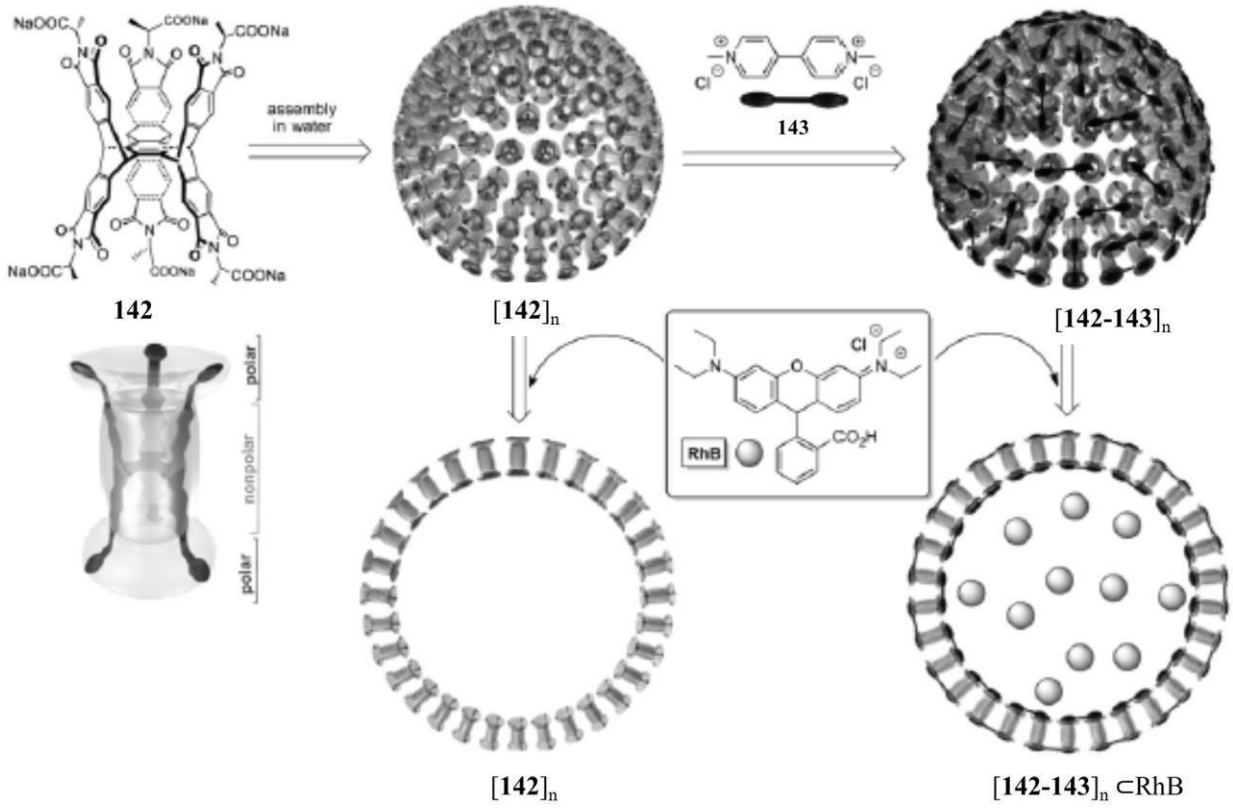

Fig. 21. Bolaamphiphilic **142** assembles into unilamellar vesicles [**142**]$_n$, which in the presence of paraquat **143** give vesicular [**142**−**143**]$_n$ with divalent guests covering their curved polyvalent surface in a lateral fashion. Encapsulation dynamic of **142** toward RhB (adapted with permission from ref. 141).

Dynamic and possible applications of structured dual-cavity baskets were explored in the last few years by Badjić's group [143, 144], more recently focusing on enacapsulation and delivery of anticancer agents [145, 146] for developing cooperative nano-antidotes. Recently, Sakurai's group reported preparation and characterization of chiral cyclic trilactams (+)- **144** and (−)-**144** with C_3 symmetry (Fig. 22a) [147]. Single X-ray analysis, NMR experiments, and computational calculations revealed that BCT (−)-**144** forms hydrophobic capsule-like structures through self-complementary NH···O intermolecular HBs with a small inner cavity, in both solid and solution phases (Fig. 22b). Moreover, these BCTs were investigated as liquid phase extraction materials of volatile compounds [148]. Perfume samples, involving a range of chiral odor active terpenoids such as *l*-menthol (LMT) (**145**) and methyl dihydrojasmonate (Kharismal, KRM) (**146**), were applied, and each sample before and after the liquid phase extraction was analyzed by solid phase microextraction (SPME)-gas chromatography hyphenated with mass spectrometry. On this basis, it was found that (+)- **144** exhibited significantly higher enrichment factors for several terpenoids, while (−)-**144** did not. The mode of interactions between each enantiomer and *l*-menthol and Kharismal was further investigated by molecular dynamics (MD) simulations and DFT calculations (Fig. 22c), showing the favourable interactions of enriched

substrates with (+)-**144** through noncovalent interactions, either HBs or electrostatic interactions.

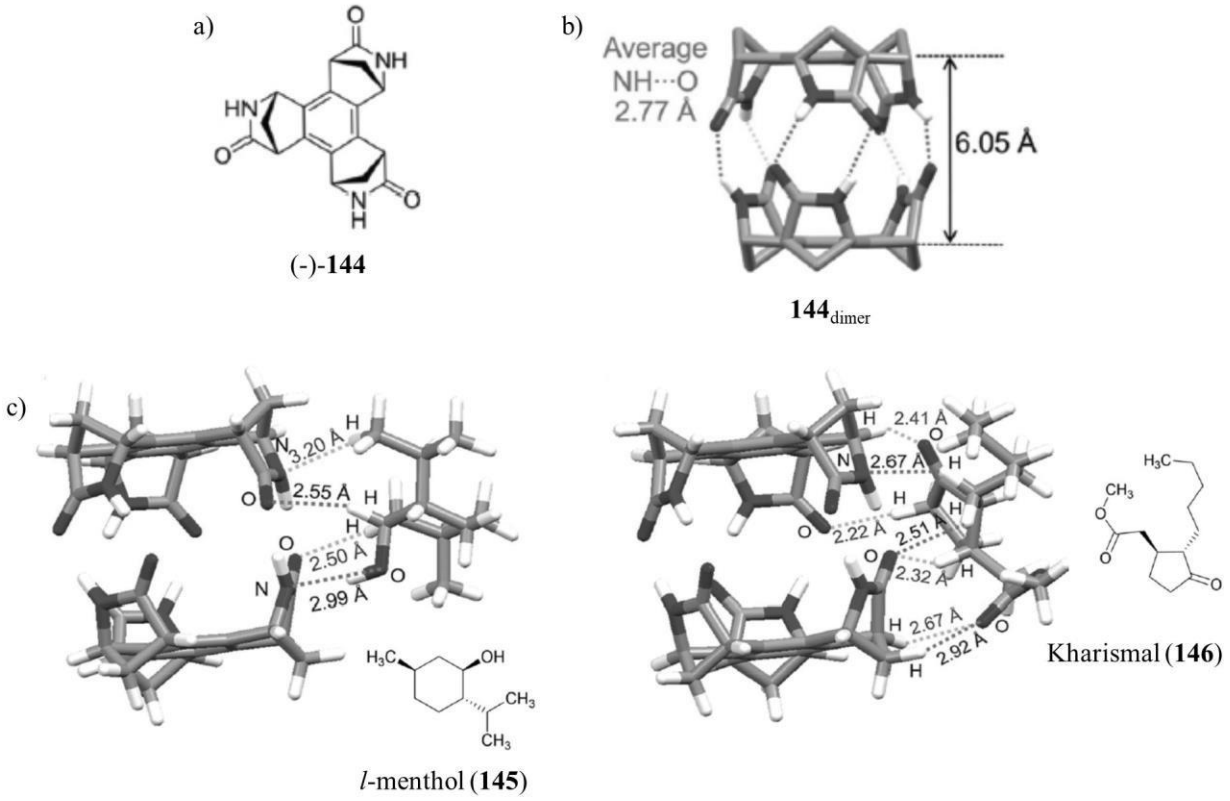

Fig. 22. a) Molecular chiral structure of (−)-**144**, b) crystal structure showing a hydrophobic capsule-like dimer consisting of two (−)-**144** molecules (**144**$_{dimer}$) via three self-complementary NH···O intermolecular HBs, and c) DFT optimized complexes (+)-**144**$_{dimer}$–LMT and (+)–**144**$_{dimer}$–KRM structures at the B3LYP-D3/6-31+G(d,p) level of theory (adapted with permission from ref. 148).

Fabris *et al*. reported about the complexation ability of *syn*-**79** toward water [149], and chiral ammonium ions [150]. In this regard, Fornili *et al*. performed analyses of 20-ns simulations of aqueous solutions of *syn*-**79**, showing that this molecule binds a single water molecule within its hydrophilic cavity for an average time interval of ca. 750 ps that is 370 times longer than the permanence time of the water around borneol [151]. Moreover, this time becomes three times longer in a 99.8% chloroform–

water solution, while it decreases for the methylether derivative of *syn*-**79** in water, becoming 279, 36 or 119 ps when one, two or all three hydroxyl hydrogen atoms are replaced by methyl groups, respectively. Finally, the oxime derivative of *syn*-**79** was shown to spontaneously bind atmospheric gases with the generation of a chiral enantiopure self-assembled dimeric capsules [152, 153].

CONCLUDING REMARKS

This review summarizes the history and evolution of bridged BCTs over five decades, highlighin gresults, findings, and concepts which have allowed this field to evolve from the pioneering low-yield syntheses of BCTs to advanced design and preparation of vesicular and nanostructured baskets and capsules for drug entrapment and delivery. Despite the fact that these applications mainly require the availability of *syn*-BCTs, recently the *anti*-isomers of BCTs based on the bicyclo[2.2.1] framework and bearing amino acid moieties at the terminations have attracted interest as stackable molecular chairs to increase the multivalency of peptides and create novel soft materials [154]. For the sake of completeness, it is worth mentioning that the bicyclo[2.2.1] framework and its natural curvature have also been fruitfully exploited in other containers such as molecular tweezers [155] and buckycatchers [156, 157], which are characterized by different topologies compared to the BTCs, but are similarly able to function as synthetic receptors in the chemical and biological environment [156-159].

CONSENT FOR PUBLICATION

Not applicable.

FUNDING

Declared none

CONFLICT OF INTEREST

The authors declare that they have no known competing financial interests or personal relationships that could have appeared to influence the work reported in this review article.

ACKNOWLEDGEMENTS

Declared none

ABBREVIATIONS

BCT Benzocyclotrimer
BuLi Butyllithium
CuTC Copper(I) thiophen-2-carboxylate
DDQ Dichlorodicyanoquinone
DFT Density functional theory
DMAD Dimethyl acetylenedicarboxylate
DMAP 4-(Dimethylamino)pyridine
DMDPE *rac*-1,2-Dimethoxy-1,2-diphenylethane
DME 1,2-Dimethoxyethane
DMF *N*,*N*-Dimethylformamide
DMPHEN Neocuproine
dppe 1,2-Bis(diphenylphosphino)ethane
ECD Electronic circular dichroism
ee Enantiomeric excess
EPS Electrostatic potential surfaces
FVP Flash vacuum pyrolysis
HB Hydrogen bond
HF Hartree-Fock
KRM Kharismal
LMT *l*-menthol
MD Molecular dynamics
m.p. Melting point
MM Molecular mechanics
NMP *N*-Methylpyrrolidinone
NMR Nucler magnetic resonance

PTAD 4-Phenyl-1,2,4-triazoline-3,5-dione
RCM Ring-closing metathesis
RhB Rhodamine
ROM Ring opening metathesis
TEM Transmission electron microscopy
THF Tetrahydrofuran
TPA Tris(2-pyridylmethyl)amine
Ts Tosyl (*p*-toluensulfonyl)

REFERENCES

[1] Purse, B.W; Rebek, J. Jr. Functional cavitands: chemical reactivity in structured environments. *Proc. Natl. Acad. Sci. USA*, **2005**, *102*, 10777–10782. DOI: 10.1073/pnas.0501731102

[2] Ballester, P.; Fujita, M.; Rebek, J. Jr. Molecular containers. *Chem. Soc. Rev.*, **2015**, *44*, 392–393. DOI: 10.1039/C4CS90101K

[3] Xiong, M.; Ding, H.; Li, B.; Zhou, T.; Wang, C. Porous organic molecular cages: from preparation to applications. *Curr. Org. Chem.*, **2014**, *18*, 1965–1972.

[4] Pérez, E.M.; Martín, N. Curves ahead: molecular receptors for fullerenes based on concave–convex complementarity. *Chem. Soc. Rev.*, **2008**, *37*, 1512–1519. DOI: 10.1039/B802589B

[5] J. Hill, T.J.; Hughes, R.K.; Scott, L.T. Steps toward the synthesis of a geodesic $C_{60}H_{12}$ end cap for a C_{3v} carbon [6,6]nanotube. *Tetrahedron*, **2008**, *64*, 11360–11369. DOI: 10.1016/j.tet.2008.09.087

[6] Saito, M.; Shinokubo, H.; Sakurai, H. Figuration of bowl-shaped π-conjugated molecules: properties and functions. *Mater. Chem. Front.*, **2018**, *2*, 635–661. DOI: 10.1039/C7QM00593H

[7] Yakiyama, Y.; Hishikawa, S.; Sakurai, H. Synthesis of C70-fragment buckybowls bearing alkoxy substituents. *Beilstein J. Org. Chem.*, **2020**, *16*, 681–690. DOI:10.3762/bjoc.16.66

[8] Chen, X.; Sakurai, H.; Wang, H.; Gao, S.; Bi, F.-D.; Bai, F.-Q. Theoretical study on the molecular stacking interactions and charge transport properties of triazasumanene crystals – from explanation to prediction. *Phys. Chem. Chem. Phys.*, **2021**, *23*, 4681–4689. DOI: 10.1039/d0cp06102f

[9] Alvi, S.; Ali, R. Synthetic approaches to bowl-shaped π-conjugated sumanene and its congeners.

892 *Beilstein J. Org. Chem.*, **2020**, *16*, 2212–2259. DOI: 10.3762/bjoc.16.186
893 [10] Barth, W.E.; Lawton, R.G. Dibenzo[ghi,mno]fluoranthene. *J. Am. Chem. Soc.*, **1966**, *88*, 380–381.
894 DOI: 10.1021/ja00954a049
895 [11] Lawton, R.G.; Barth, W.E. Synthesis of corannulene. *J. Am. Chem. Soc.*, **1971**, *93*, 1730–1745.
896 DOI: 10.1021/ja00736a028
897 [12] Butterfield, A.M.; Gilomen, B.; Siegel, J.S. Kilogram-scale production of corannulene. *Org.*
898 *Process Res. Dev.*, **2012**, *16*, 664−676. DOI: 10.1021/op200387s
899 [13] Higashibayashi, S.; Onogi, S.; Srivastava, H.K.; Sastry, G.N.; Wu, Y.–T.; Sakurai, H.
900 Stereoelectronic effect of curved aromatic structures: favoring the unexpected *endo* conformation
901 of benzylic-substituted sumanene. *Angew. Chem. Int. Ed.*, **2013**, *52*, 7314–7316. DOI:
902 10.1002/anie.201303134
903 [14] Seiders, T.J.; Baldridge, K.K.; Grube, G.H.; Siegel, J.S. Structure/energy correlation of bowl depth
904 and inversion barrier in corannulene derivatives: combined experimental and quantum mechanical
905 analysis. *J. Am. Chem. Soc.*, **2001**, *123*, 517–525. DOI: 10.1021/ja0019981
906 [15] Kang, J.; Miyajima, D.; Itoh, Y.; Mori, T.; Tanaka, H.; Yamauchi, M.; Inoue, Y.; Harada, S.; Aida,
907 T. C_5-Symmetric chiral corannulenes: desymmetrization of bowl inversion equilibrium via
908 "intramolecular" hydrogen-bonding network. *J. Am. Chem. Soc.*, **2014**, *136*, 10640−10644. DOI:
909 10.1021/ja505941b
910 [16] Juríček, M.; Strutt, N.L.; Barnes, J.C.; Butterfield, A.M.; Dale, E.J.; Baldridge, K.K.; Stoddart,
911 J.F.; Siegel, J.S. Induced-fit catalysis of corannulene bowl-to-bowl inversion. *Nat. Chem.*, **2014**, *6*,
912 222–228. DOI: 10.1038/nchem.1842
913 [17] Nestoros, E.; Stuparu, M.C. Corannulene: a molecular bowl of carbon with multifaceted properties
914 and diverse applications. *Chem. Commun.*, **2018**, *54*, 6503–6519. DOI: 10.1039/C8CC02179A
915 [18] Shrestha, B.B.; Karanjit, S.; Higashibayashi, S.; Sakurai, H. Correlation between bowl-inversion
916 energy and bowl depth in substituted sumanenes. *Pure Appl. Chem.*, **2014**, *86*, 747–753. DOI:

10.1515/pac-2013-1212

[19] Kanagaraj, K.; Lin, K.; Wu, W.; Gao, G.; Zhong, Z.; Su, D.; Yang, C. Chiral buckybowl molecules. *Symmetry*, **2017**, *9*, 174. DOI: 10.3390/sym9090174

[20] Fabris, F.; Zonta, C.; Borsato, G.; De Lucchi, O. Benzocyclotrimers: from the Mills-Nixon effect to gas hosting. *Acc. Chem. Res.*, **2011**, *44*, 416–423. DOI: 10.1021/ar100128s

[21] Guo, C.; Xia, D.; Yang, Y.; Zuo, X. Synthesis of π-conjugated benzocyclotrimers. *Chem. Rec.*, **2019**, *19*, 2143–2156. DOI: 10.1002/tcr.201800160

[22] Scott, L.T.; Matthew S. Bratcher, M.S.; Hagen, S. Synthesis and characterization of a $C_{36}H_{12}$ fullerene subunit. *J. Am. Chem. Soc.*, **1996**, *118*, 8743–8744. DOI: 10.1021/ja9621511

[23] Ansems, B.M.; T. Scott, L.T. Circumtrindene: A geodesic dome of molecular dimensions. Rational synthesis of 60% of C_{60}. *J. Am. Chem. Soc.*, **2000**, *122*, 2719–2724. DOI: 10.1021/ja993028n

[24] Buess, C.M.; Lawson, D.D. The preparation, reactions, and properties of triphenylenes. *Chem. Rev.*, **1960**, *60*, 313–330. DOI: 10.1021/cr60206a001

[25] Ho, D.M.; Pascal, R.A. Jr. Decacyclene: a molecular propeller with helical crystals. *Chem. Mater.*, **1993**, *5*, 1358–1361. DOI: 10.1021/cm00033a029

[26] Baillargeon, P.; Dory, Y.L. Rational design and gas-phase characterization of molecular capsules by self-assembly of a symmetric hexasubstituted benzene with seven-membered lactams. *J. Am. Chem. Soc.*, **2008**, *130*, 5640–5641. DOI: 10.1021/ja800734b

[27] Carrillo, R.; Martín, T.; López-Rodríguez, M.; Crisóstomo, F.P. Expedient synthesis of C_3-symmetric hexasubstituted benzenes via Nicholas reaction/[2 + 2 + 2] cycloaddition. New platforms for molecular recognition. *Org. Lett.*, **2014**, *16*, 552–555. DOI: 10.1021/ol403428p

[28] Carrillo, R.; Hynes, M.J.; Martín, V.S.; Martín, T.; Crisóstomo, F.P. Synthesis of new benzocyclotrimer analogues: new receptors for tetramethylammonium ion recognition. *Org. Lett.*,

2015, *17*, 2912–2915. DOI: 10.1021/acs.orglett.5b01058

[29] Borges-González, J.; Martín, T. Efficient synthesis of benzocyclotrimer analogues by Negishi cross-coupling and intramolecular nucleophilic substitution. *Chem. Commun.*, **2018**, *54*, 362–365. DOI: 10.1039/C7CC08616D

[30] Sakurai, H.; Daiko, T.; Hirao, T. A Synthesis of sumanene, a fullerene fragment. *Science*, **2003**, *301*, 1878. DOI: 10.1126/science.1088290

[31] Schröder, G.; Oth, J. F. M. Recent chemistry of bullvalene. *Angew. Chem. Internat. Edit.*, **1967**, *6*, 414–423. DOI: 10.1002/anie.196704141

[32] Huebner, C.F.; Puckett, R.T.; Brzechffa, M.; Schwartz, S.L. A trimeric $C_{48}H_{30}$ hydrocarbon of unusual structural interest derived from 9,10-dihydro-9,10-ethenoanthracene. *Tetrahedron Lett.*, **1970**, 359–362. DOI: 10.1016/0040-4039(70)80084-3

[33] Baldridge, K.K.; Siegel, J.S. Bond alternation in triannelated benzenes: dissection of cyclic π from "Mills-Nixon" effect. *J. Am. Chem. Soc.*, **1992**, *114*, 9583–9587. DOI: 10.1021/ja00050a043

[34] Ashton, P.R.; Brown, G.R.; Isaacs, N.S.; Giuffrida, D.; Kohnke, F.H.; Mathias, J.P.; Slawin, A.M.Z.; Smith, D.R.; Stoddart, J.F.; Williams, D.J. Molecular LEGO. 1. Substrate-directed synthesis via stereoregular Diels-Alder oligomerizations. *J. Am. Chem. Soc.*, **1992**, *114*, 6330–6353. DOI: 10.1021/ja00042a009

[35] Ashton, P.R.; Girreser, U.; Giuffrida, D.; Kohnke, F.H.; Mathias, J.P.; Raymo, F.M.; Slawin, A.M.Z.; Stoddart, J.F.; Williams, D.J. Molecular belts. 2. Substrate-directed synthese of belt-type and cage-type structures. *J. Am. Chem. Soc.*, **1993**, *115*, 5422–5429. DOI: 10.1021/ja00066a010

[36] Shahlai, K.; Hart, H. The mechanism of trimerization of bicyclo[2.2.2]alkynes. *J. Am. Chem. Soc.*, **1988**, *110*, 7136–7140. DOI: 10.1021/ja00229a029

[37] Cossu, S.; Cimenti, C.; Peluso, P.; Paulon, A.; De Lucchi, O. Enantiomeric discrimination in a reiterative domino coupling process: CuI-mediated syn cyclotrimerization of racemic polycyclic trimethylstannyl bromonorbornadienes. *Angew. Chem. Int. Ed.*, **2001**, *40*, 4086–4089. DOI:

10.1002/1521-3773(20011105)40:21<4086::AID-ANIE4086>3.0.CO;2-5

[38] Higashibayashi, S.; Sakurai, H. Synthesis of an enantiopure *syn*-benzocyclotrimer through regio-selective cyclotrimerization of a halonorbornene derivative under palladium nanocluster conditions. *Chem. Lett.*, **2007**, *36*, 18–19. DOI: 10.1246/cl.2007.18

[39] Lei, Z.; Gunther, M.J.; Gunawardana, V.W.L.; Pavlović, R.Z.; Xie, H.; Zhu, X.; Keenan, M.; Riggs, A.; Badjić, J.D. A highly diastereoselective synthesis of deep molecular baskets. *Chem. Commun.*, **2020**, *56*, 10243–10246. DOI: 10.1039/D0CC04650G

[40] Rieth, S.; Hermann, K.; Wang, B.–Y.; Badjić, J.D. Controlling the dynamics of molecular encapsulation and gating. *Chem. Soc. Rev.*, **2011**, *40*, 1609–1622. DOI: 10.1039/C005254J

[41] Lei, Z.; Finnegan, T.J.; Gunawardana, V.W.L.; Pavlović, R.Z.; Xie, H.; Moore, C.E.; Badjić, J.D. A molecular capsule with revolving doors partitioning its inner space. *Chem. Eur. J.* **2020**, *26*, 16480–16485. DOI: 10.1002/chem.202003247

[42] Hart, H.; Shamouilian, S.; Takehira, Y. Generalization of the triptycene concept. Use of diaryne equivalents in the synthesis of iptycenes. *J. Org. Chem.*, **1981**, *46*, 4427−4432. DOI: 10.1021/jo00335a021

[43] Sing, S.B.; Hart, H. Extensions of bicycloalkyne trimerizations. *J. Org. Chem.*, **1990**, *55*, 3412−3415. DOI: 10.1021/jo00297a086

[44] Gassman, P.G.; Gennick, I. Synthesis and reactions of 2-lithio-3-chlorobicyclo[2.2.1]hept-2-ene. Generation of the trimer of bicyclo[2.2.1]hept-2-yne. *J. Am. Chem. Soc.*, **1980**, *102*, 6863−6864. DOI: 10.1021/ja00542a041

[45] Komatsu, K.; Jinbu, Y.; Gillette, G.R.; West, R. Facile synthesis, crystal structure, and oxidizability of novel benzene tris-annelated with bicyclo[2.2.2]oct-2-ene. *Chem. Lett.*, **1988**, 2029−2032. DOI: 10.1246/cl.1988.2029

[46] Komatsu, K.; Akamatsu, H.; Jinbu, Y.; Okamoto, K. 1,2:3,4:5,6-Tris(bicyclo[2.2.2]octeno)tropylium ion: an all-hydrocarbon carbocation with extraordinary

stability. *J. Am. Chem. Soc.*, **1988**, *110*, 633−634. DOI: 10.1021/ja00210a072

[47] Komatsu, K.; Aonuma, S.; Jinbu, Y.; Tsuji, R.; Hirosawa, C.; Takeuchi, K. Generation and oligomerization of bicyclo[2.2.2]octyne and properties of tris(bicyclo[2.2.2]octeno)benzene obtained from the linear trimer. *J. Org. Chem.*, **1991**, *56*, 195−203. DOI: 10.1021/jo00001a039

[48] Matsuura, A.; Nishinaga, T.; Komatsu, K. Reactions of novel benzyne annelated with two bicyclo[2.2.2]octene units. *Tetrahedron Lett.*, **1997**, *38*, 4125−4128. DOI: 10.1016/S0040-4039(97)00842-3

[49] Frank, N.L.; Baldridge, K.K.; Siegel, J.S. Synthesis and characterization of trisbicyclo[2.1.1]hexabenzene, a highly strained bicycloannelated benzene. *J. Am. Chem. Soc.*, **1995**, *117*, 2102−2103. DOI: 10.1021/ja00112a028

[50] Durr, R.; De Lucchi, O.; Cossu, S.; Lucchini, V. *syn*- and *anti*-Benzotris(norbornadiene)s. *Chem. Commun.*, **1996**, 2247−2248. DOI: 10.1039/CC9960002447

[51] Cossu, S.; De Lucchi, O.; Lucchini, V.; Valle, G.; Balci, M.; Dastan, A.; Demirci, B. Synthesis of 2,3-dibromobenzonorbornadiene and its cyclotrimerization into 5,18:6,11:12,17-trimethanotrinaphthylene. *Tetrahedron Lett.*, **1997**, *38*, 5319−5322. DOI: 10.1016/S0040-4039(97)01162-3

[52] Zonta, C.; Cossu, S.; Peluso, P.; De Lucchi, O. Stereochemistry of the cyclotrimerization of enantiopure polycyclic bromostannylalkenes: mechanistic considerations on the coupling of alkenyl stannanes by Copper(II) nitrate. *Tetrahedron Lett.*, **1999**, *40*, 8185−8188. DOI: 10.1016/S0040-4039(99)01736-0

[53] Fabris, F.; De Martin, A; De Lucchi, O. The cyclotrimerization of (+)-camphor. *Tetrahedron Lett.*, **1999**, *40*, 9121−9124. DOI: 10.1016/S0040-4039(99)01889-4

[54] Mills, W.H.; Nixon, I.G. CCCXXXII. Stereochemical influences on aromatic substitution. Substitution derivatives of 5-hydroxyhydrindene. *J. Chem. Soc.*, **1930**, 2510−2524. DOI: 10.1039/JR9300002510

[55] Frank, N.L.; Siegel, J.S. In: *Advances in Theoretically Interesting Molecules*; Thummel, R.P., Ed.; Elsevier: Amsterdam, 1995; Vol. 3, pp. 209−260.

[56] Lin, X.; Chen, Z.; Wu, W. The driving force for π-bond localization and bond alternation in trisannelated benzenes. *Phys. Chem. Chem. Phys.*, **2017**, *19*, 3019−3027. DOI: 10.1039/C6CP06915K

[57] Ermer, O. Concerning the structure of benzene. *Angew. Chem. Int. Ed.*, **1987**, *26*, 782−784. DOI: 10.1002/anie.198707821

[58] Stanger, A. Is the Mills-Nixon effect real? *J. Am. Chem. Soc.*, **1991**, *113*, 8277−8280. DOI: 10.1021/ja00022a012

[59] Siegel, J.S. Mills-Nixon effect: wherefore art thou? *Angew. Chem. Int. Ed. Engl.*, **1994**, *33*, 1721−1723. DOI: 10.1002/anie.199417211

[60] Bürgi, H.−B; Baldridge, K.K.; Hardcastle, K.; Frank, N.L.; Gantzel, P.; Siegel, J.S.; Ziller, J. X-ray diffraction evidence for a cyclohexatriene motif in the molecular structure of tris(bicyclo[2.1.1]hexeno)benzene: bond alternation after the refutation of the Mills-Nixon theory. *Angew. Chem. Int. Ed. Engl.*, **1995**, *34*, 1454−1456. DOI: 10.1002/anie.199514541

[61] Shaik, S.; Shurki, A.; Danovich, D.; Hiberty, P.C. A different story of π-delocalization – The distortivity of π-electrons and its chemical manifestations. *Chem. Rev.*, **2001**, *101*, 1501−1539. DOI: 10.1021/cr990363l

[62] Jemmis, E.D.; Kiran, B. Bond localization in annelated benzenes: an additivity scheme. *J. Org. Chem.*, **1996**, *61*, 9006−9008. DOI: 10.1021/jo9612842

[63] Shurki, A.; Shaik, S. The distortive tendency of benzene π electrons: how is it related to structural observables? *Angew. Chem. Int. Ed. Engl.*, **1997**, *36*, 2205−2206. DOI: 10.1002/anie.199722051

[64] Rouhi, A.M. Scientists localize benzene's electrons, trap elusive cyclohexatriene motif. *Chem. Eng. News*, **1996**, 74, 27–31. DOI: 10.1021/cen-v074n014.p027

[65] Rathore, R.; Loyd, S. H.; Kochi, J. K. Isolation, structure, and reactivity of a novel chloro-arenium cation for electrophilic (transfer) chlorinations. *J. Am. Chem. Soc.*, **1994**, *116*, 8414–8415. DOI:

10.1021/ja00097a078

[66] Rathore, R.; Kochi, J. K. Isolation of novel radical cations from hydroquinone ethers. conformational transition of the methoxy group upon electron transfer. *J. Org. Chem.*, **1995**, *60*, 4399–4411. DOI: 10.1021/jo00119a017

[67] Venugopalan, P.; Bürgi, H.-B; Frank, N.L.; Baldridge, K.K.; Siegel, J.S. The crystal structure of a heptiptycene-chlorobenzene clathrate. *Tetrahedron Lett.*, **1995**, *36*, 2419−2422. DOI: 10.1016/0040-4039(95)00318-7

[68] Frank, N.L.; Baldridge, K.K.; Gantzel, P.; Siegel, J.S. Partial bond localization in the crystal structure of trisbicyclo[2.2.1]heptabenzene and its effect on Cr-arene dynamics. *Tetrahedron Lett.*, **1995**, *36*, 4389−4392. DOI: 10.1016/0040-4039(95)00857-9

[69] Hunter, G.; MacKay, R. L.; Kremminger, P.; Weissensteiner, W. Observation of slowed rotation about the η^6-arene-chromium bond in the tripodal chromium complexes of the trimers of bicyclo[2.2.1]hept-2-yne: intramolecular rotational barriers in organometallic complexes and their correlation with internal non-bonding interactions and structural changes. *J. Chem. Soc. Dalton Trans.*, **1991**, 3349−3358. DOI: 10.1039/DT9910003349

[70] Nambu, M.; Siegel, J. S. An induced barrier to rotation about the η^6-arene-metal bond in centrally bound bent-terphenylenechromium tricarbonyl: a gauge for aromatic character and bond localization? *J. Am. Chem. Soc.*, **1988**, *110*, 3675−3676. DOI: 10.1021/ja00219a061

[71] Cardullo, F.; Giuffrida, D.; Kohnke, F.H.; Raymo, F.M.; Stoddart, J.F.; Williams, D.J. Effects of strained bicyclic annelation on the benzene nucleus: the X-ray crystal structures of a triphenylene and two anthracene derivatives. *Angew. Chem. Int. Ed. Engl.*, **1996**, *35*, 339−341. DOI: 10.1002/anie.199603391

[72] Pozo, I.; Guitián, E.; Pérez, D.; Peña, D. Synthesis of nanographenes, starphenes, and sterically congested polyarenes by aryne cyclotrimerization. *Acc. Chem. Res.*, **2019**, *52*, 2472−2481. DOI: 0.1021/acs.accounts.9b00269

[73] Paquette, L.A.; Moorhoff, C.M.; Maynard, G.D.; Hickey, E.R.; Rogers, R.D. Stereochemical course of the base-promoted aldol self-coupling of racemic 5-norbornen-2-one and 2-norbornanone. *J. Org. Chem.*, **1991**, *56*, 2449−2455. DOI: 10.1021/jo00007a036

[74] Reza, A.F.G.M.; Higashibayashi, S.; Sakurai, H. Preparation of C_3-symmetric homochiral *syn*-trisnorbornabenzenes through regioselective cyclotrimerization of enantiopure iodonorbornenes. *Chem. Asian J.*, **2009**, *4*, 1329−1337. DOI: 10.1002/asia.200900132

[75] Durr, R.; Cossu, S.; Lucchini, V.; De Lucchi, O. Trisannelated benzenes by cyclotrimerization of bromostannylalkenes. *Angew. Chem. Int. Ed. Engl.*, **1997**, *36*, 2805–2807. DOI: 10.1002/anie.199728051

[76] Zonta, C.; Cossu, S.; De Lucchi, O. Synthesis of benzotri(benzonorbornadienes) (BTBNDs): Rigid, cup-shaped molecules with high electron density within the cavity. *Eur. J. Org. Chem.*, **2000**, 1965–1971. DOI: 10.1002/(SICI)1099-0690(200005)2000:10<1965::AID-EJOC1965>3.0.CO;2-C

[77] Piers, E.; Gladstone, P.L.; Yee, J.G.K.; McEachern, E.J. Intermolecular homocoupling of alkenyltrimethylstannane functions mediated by CuCl: preparation of functionalized conjugated diene and tetraene systems. *Tetrahedron*, **1998**, *54*, 10609-10626. DOI: 10.1016/S0040-4020(98)00592-4

[78] Peluso, P.; De Lucchi, O.; Cossu, S. Role of copper in the stereoselective metal-promoted cyclotrimerization of polycyclic alkenes. *Eur. J. Org. Chem.*, **2002**, 4032–4036. DOI: 10.1002/1099-0690(200212)2002:23<4032::AID-EJOC4032>3.0.CO;2-X

[79] Border, S. E.; Pavlovic, R. Z.; Zhiquan, L.; Badjic, J. D. Removal of nerve agent simulants from water using light-responsive molecular baskets. *J. Am. Chem. Soc.*, **2017**, *139*, 18496−18499. DOI: 10.1021/jacs.7b11960

[80] Gunther, M.J.; Pavlović, R.Z.; Fernandez, J.P.; Zhiquan, L.; Gallucci, J.; Hadad, C.M.; Badjić, J.D. Stereo- and regioselective synthesis of molecular baskets. *J. Org. Chem.*, **2019**, *84*, 4392−4401. DOI: 10.1021/acs.joc.9b00330

[81] Matsuura, A.; Komatsu, K. Efficient synthesis of benzene and planar cyclooctatetraene fully annelated with bicyclo[2.2.1]hex-2-ene. *J. Am. Chem. Soc.*, **2001**, *123*, 1768–1769. DOI: 10.1021/ja015156t

[82] Borsato, G.; De Lucchi, O.; Fabris, F.; Groppo, L.; Lucchini, V.; Zambon, A. Efficient cyclotrimerization of bicyclic *vic*-bromostannylalkenes promoted by copper(I) thiophen-2-carboxylate. *J. Org. Chem.*, **2002**, *67*, 7894–7897. DOI: 10.1021/jo020396s

[83] Allred, G. D.; Liebeskind, L. S.; Sanford, S. Copper-mediated cross-coupling of organostannanes with organic iodides at or below room temperature. *J. Am. Chem. Soc.*, **1996**, *118*, 2748–2749. DOI: 10.1021/ja9541239

[84] Zhang, S.; Zhang, D.; Liebeskind, L. S. Ambient temperature, Ullmann-like reductive coupling of aryl, heteroaryl, and alkenyl halides. *J. Org. Chem.*, **1997**, *62*, 2312–2313. DOI: 10.1021/jo9700078

[85] Fabris, F.; Zambrini, L.; Rosso, E.; De Lucchi, O. Comparative cyclotrimerization of enantiopure *vic*-bromo(trimethylstannyl)bicycloalkenes derived from (+)-camphor, (+)-fenchocamphorone and (-)-epicamphor: effect of the bridgehead methyl group on the *syn*/*anti* product ratio. *Eur. J. Org. Chem.*, **2004**, 3313–3322. DOI: 10.1002/ejoc.200400120

[86] Fabris, F.; Bellotto, L.; De Lucchi, O. (+)-*syn*-benzotriborneol: the first functionalized enantiopure C_3-symmetric benzocyclotrimer. *Tetrahedron Lett.*, **2003**, *44*, 1211−1213. DOI: 10.1016/S0040-4039(02)02789-2

[87] Mazzeo, G.; Giorgio, E.; Rosini, C.; Fabris, F.; Fregonese, E.; Toniolo, U.; De Lucchi, O. Synthesis, chiroptical properties, and their theoretical simulation of some highly rotating benzotricamphor derivatives. *Chirality*, **2009**, *21*, E86−E97. DOI: 10.1002/chir.20780

[88] Borsato, G.; De Lucchi, O.; Fabris, F.; Lucchini, V.; Pasqualotti, M.; Zambon, A. Synthesis of the *syn* and *anti* isomer of 1,4,5,8,9,12-hexahydro-2,3,6,7,10,11-hexamethylidene-1,4:5,8:9,12-trimethanotriphenylene and Diels-Alder reactivity of the *syn* isomer. *Tetrahedron Lett.*, **2003**, *44*, 561−563. DOI: 10.1016/S0040-4039(02)02533-9

[89] Dalkiliç, E.; Güney, M.; Daştan, A.; Saracoglu, N.; De Lucchi, O.; Fabris, F. Novel and versatile protocol for the preparation of functionalized benzocyclotrimers. *Tetrahedron Lett.*, **2009**, *50*, 1989–1991. DOI: 10.1016/j.tetlet.2009.02.070

[90] Maslak, V.; Yan, Z.; Xia, S.; Gallucci, J.; Hadad, C.M.; Badjić, J.D. Design, synthesis, and conformational dynamics of a gated molecular basket. *J. Am. Chem. Soc.*, **2006**, *128*, 5887–5894. DOI: 10.1021/ja060534l

[91] Borsato, G.; Brussolo, S.; Crisma, M.; De Lucchi, O.; Lucchini, V.; Zambon, A. Tris-annelated benzenes selectively perfunctionalized on one side only: hexachlorobenzotrinorbornadiene as a versatile scaffold for the constructiion of molecular domes. *Synlett*, **2005**, *7*, 1125−1128. DOI: 10.1055/s-2005-865215

[92] Borsato, G.; Crisma, M.; De Lucchi, O.; Lucchini, V.; Zambon, A. “Hexacarboxytrindanes”: benzene rings with homotopic faces as scaffolds for the construction of D_3 chiral architectures. *Angew. Chem. Int. Ed.*, **2005**, *44*, 7435−7439. DOI: 10.1002/anie.200502262

[93] De Lucchi, O.; Daştan, A.; Altundaş, A.; Fabris, F.; Balci, M. Cyclotrimerization of 'oxabenzonorbornadiene': synthesis of *syn*- and *anti*-5,6,11,12,17,18-hexahydro-5,18:6,11:12,17-triepoxytrinaphthylene. *Helv. Chim. Acta*, **2004**, *87*, 2364–2367. DOI: 10.1002/hlca.200490213

[94] Zonta, C.; Fabris, F.; De Lucchi, O. The pyrrole approach toward the synthesis of fully functionalized cup-shaped molecules. *Org. Lett.*, **2005**, *7*, 1003–1006. DOI: 10.1021/ol047569f

[95] Rathore, R.; Lindeman, S.V.; Kumar, A.S.; Kochi, J.K. Novel synthesis and structures of tris-annelated benzene donors for the electron-density elucidation of the classical Mills-Nixon effect. *J. Am. Chem. Soc.*, **1998**, *120*, 6012–6018. DOI: 10.1021/ja980805v

[96] Stille, J.K. The palladium-catalyzed cross-coupling reactions of organotin reagents with organic electrophiles. *Angew. Chem. Int. Ed. Engl.*, **1986**, *25*, 508–524. DOI: 10.1002/anie.198605081

[97] Paulon, A.; Cossu, S.; De Lucchi, O.; Zonta, C. Palladium-catalysed cyclotrimerization reactons of polycyclic alkenes under the Stille and Grigg coupling conditions. *Chem. Commun.*, **2000**, 1837–1838. DOI: 10.1039/B006698M

[98] Grigg, R.; Teasdale, A.; Sridharan, V. Palladium catalysed intramolecular coupling of aryl and benzylic halides and related tandem cyclisations. A simple synthesis of hippadine. *Tetrahedron Lett.*, **1991**, *32*, 3859–3862. DOI: 10.1016/S0040-4039(00)79397-X

[99] Cossu, S.; De Lucchi, O.; Paulon, A.; Peluso, P.; Zonta, C. *anti*-Selective Heck-type cyclotrimerization of polycyclic bromoalkenes. *Tetrahedron Lett.*, **2001**, *42*, 3515–3518. DOI: 10.1016/S0040-4039(01)00495-6

[100] Beletskaya, I.P.; Cheprakov, A.V. The Heck reaction as a sharpening stone of palladium catalysis. *Chem. Rev.*, **2000**, *100*, 3009–3066. DOI: 10.1021/cr9903048

[101] Zambrini, L.; Fabris, F.; De Lucchi, O.; Gardenal, G.; Visentin, F.; Canovese, L. Heck self-condensation of polycyclic haloalkenes: the case of (1*R*)-2-iodobornene. *Tetrahedron*, **2001**, *57*, 8719–8724. DOI: 10.1016/S0040-4020(01)00850-X

[102] Higashibayashi, S.; Sakurai, H. Asymmetric synthesis of a chiral buckybowl, trimethylsumanene. *J. Am. Chem. Soc.*, **2008**, *130*, 8592−8593. DOI: 10.1021/ja802822k

[103] Tan, Q.; Higashibayashi, S.; Karanjit, S.; Sakurai, H. Enantioselective synthesis of a chiral nitrogen doped buckybowl. *Nat. Commun*, **2012**, *3*, 891. DOI: 10.1038/ncomms1896

[104] Higashibayashi, S.; Reza, A.F.G.M.; Sakurai, H. Stereoselective cyclotrimerization of enantiopure iodonorbornenes catalyzed by Pd nanoclusters for C_3 or C_{3v} symmetric *syn*-tris(norborneno)benzenes. *J. Org. Chem.*, **2010**, *75*, 4626−4628. DOI: 10.1021/jo100710h

[105] Kasprzak, A.; Kowalczyk, A.; Jagielska, A.; Wagner, B.; Nowicka, A.M.; Sakurai, H. Tris(ferrocenylmethidene)sumanene: synthesis, photophysical properties and applications for

efficient caesium cation recognition in water. *Dalton Trans.*, **2020**, *49*, 9965–9971. DOI: 10.1039/d0dt01506g.

[106] Sakurai, H. The dawn of sumanene chemistry: my personal history with π-figuration. *Bull. Chem. Soc. Jpn.*, **2021**. DOI: 10.1246/bcsj.20210046

[107] Yamanaka, M.; Morishima, M.; Shibata, Y.; Higashibayashi, S.; Sakurai, H. DFT Studies of mechanism and origin of stereoselectivity of palladium-catalyzed cyclotrimerization reactions affording *syn*-tris(norborneno)benzenes. *Organometallics*, **2014**, *33*, 3060–3068. DOI: 10.1021/om500322b

[108] Yan, Z.; McCracken, T.; Xia, S.; Maslak, V.; Gallucci, J.; Hadad, C.M.; Badjić, J.D. Supramolecular catalysis at work: diastereoselective synthesis of a molecular bowl with dynamic inner space. *J. Org. Chem.*, **2008**, *73*, 355−363. DOI: 10.1021/jo701538g

[109] Rathore, R.; Lindeman, S.V.; Kochi, J.K. Charge-transfer probes for molecular recognition via steric hindrance in donor-acceptor pairs. *J. Am. Chem. Soc.*, **1997**, *119*, 9393−9404. DOI: 10.1021/ja9720319

[110] Ashton, P.R.; Isaacs, N.S.; Kohnke, F.H.; d'Alcontes, G.S.; Stoddart, J.F. Trinacrene – a product of structure-directed synthesis. *Angew. Chem. Int. Ed. Engl.*, **1989**, *28*, 1261–1263. DOI: 10.1002/anie.198912611

[111] Mastalerz, M. Shape-persistent organic cage compounds by dynamic covalent bond formation. *Angew. Chem. Int. Ed.*, **2010**, *49*, 5042–5053. DOI: 10.1002/anie.201000443

[112] Shi, J.; Li, Y.; Li, Y. Aryne multifunctionalization with benzdiyne and benztriyne equivalents. *Chem. Soc. Rev.*, **2017**, *46*, 1707–1719. DOI: 10.1039/c6cs00694a

[113] Kamieth, M.; Klärner, F.–G.; Diederich, F. Modeling the supramolecular properties of aliphatic-aromatic hydrocarbons with convex–concave topology. *Angew. Chem. Int. Ed.*, **1998**, *37*, 3303–3306. DOI: 10.1002/(SICI)1521-3773(19981217)37:23<3303::AID-ANIE3303>3.0.CO;2-T

[114] Zhou, H.–X.; Wlodek, S.T.; McCammon, J.A. Conformation gating as a mechanism for enzyme specificity. *Proc. Natl. Acad. Sci. USA*, **1998**, *95*, 9280–9283. DOI: 10.1073/pnas.95.16.9280

[115] Hermann, K.; Ruan, Y.; Hardin, A.M.; Hadad, C.M.; Badjić, J.D. Gated molecular baskets. *Chem. Soc. Rev.*, **2015**, *44*, 500–514. DOI: 10.1039/C4CS00140K

[116] Wang, B.–Y.; Bao, X.; Stojanović, S.; Hadad, C.M.; Badjić, J.D. Encapsulation of guests within a gated molecular basket: thermodynamics and selectivity. *Org. Lett.*, **2008**, *10*, 5361–5364. DOI: 10.1021/ol802199t

[117] Wang, B.–Y.; Bao, X.; Yan, Z.; Maslak, V.; Hadad, C.M.; Badjić, J.D. A 3-fold "butterfly valve" in command of the encapsulation's kinetic stability. Molecular baskets at work. *J. Am. Chem. Soc.*, **2008**, *130*, 15127–15133. DOI: 10.1021/ja8041977

[118] Rieth, S.; Wang, B.–Y.; Bao, X.; Badjić, J.D. Four-state switching characteristics of a gated molecular basket. *Org. Lett.*, **2009**, *11*, 2495–2498. DOI: 10.1021/ol9009392

[119] Wang, B.–Y.; Rieth, S.; Badjić, J.D. Tuning the rate of molecular translocation. *J. Am. Chem. Soc.*, **2009**, *131*, 7250–7252. DOI: 10.1021/ja9023868

[120] Rieth, S.; Bao, X.; Wang, B.–Y.; Hadad, C.M.; Badjić, J.D. Gated molecular recognition and dynamic discrimination of guests. *J. Am. Chem. Soc.*, **2010**, *132*, 773–776. DOI: 10.1021/ja908436c

[121] Bao, X.; Rieth, S.; Stojanović, S.; Hadad, C.M.; Badjić, J.D. Molecular recognition of a transition state. *Angew. Chem. Int. Ed.*, **2010**, *49*, 4816–4819. DOI: 10.1002/anie.201000656

[122] Rieth, S.; Badjić, J.D. The effect of the dynamics of revolving gates on the kinetics of molecular encapsulation – The activity/selectivity relationship. *Chem. Eur. J.*, **2011**, *17*, 2562–2565. DOI: 10.1002/chem.201003138

[123] Hermann, K.; Rieth, S.; Taha, H.A.; Wang, B.–Y.; Hadad, C.M.; Badjić, J.D. On the mechanism of action of gated molecular baskets: The synchronicity of the revolving motion of gates and in/out trafficking of guests. *Beilstein J. Org. Chem.*, **2012**, *8*, 90–99. DOI:10.3762/bjoc.8.9

[124] Yan, Z.; Xia, S.; Gardlik, M.; Seo, W.; Maslak, V.; Gallucci, J.; Hadad, C.M.; Badjić, J.D. Silver(I) mediated folding of a molecular basket. *Org. Lett.*, **2007**, *9*, 2301–2304. DOI: 10.1021/ol0705595

[125] Rieth, S.; Yan, Z.; Xia, S.; Gardlik, M.; Chow, A.; Fraenkel, G.; Hadad, C.M.; Badjić, J.D. Molecular encapsulation via metal-to-ligand coordination in a Cu(I)-folded molecular basket. *J. Org. Chem.*, **2008**, *73*, 5100–5109. DOI: 10.1021/jo800748k

[126] Gardlik, M.; Yan, Z.; Xia, S.; Rieth, S.; Gallucci, J.; Hadad, C.M.; Badjić, J.D. A close inspection of Ag(I) coordination to molecular baskets. A study of solvation and guest encapsulation in solution and the solid state. *Tetrahedron*, **2009**, *65*, 7213–7219. DOI: 10.1016/j.tet.2008.11.098

[127] Stojanović, S.; Turner, D.A.; Hadad, C.M.; Badjić, J.D. Controlling dynamic stereoisomerism in transition-metal folded baskets. *Chem. Sci.*, **2011**, *2*, 752–759. DOI: 10.1039/c0sc00592d

[128] Zhiquan, L.; Polen, S.; Hadad, C.M.; RajanBabu, T.V.; Badjić, J.D. Russian nesting doll complexes of molecular baskets and zinc containing TPA ligands. *J. Am. Chem. Soc.*, **2016**, *138*, 8253−8258. DOI: 10.1021/jacs.6b04436

[129] Zhiquan, L.; Polen, S.M.; Hadad, C.M.; RajanBabu, T.V.; Badjić, J.D. Examining the scope and thermodynamics of assembly in nesting complexes comprising molecular baskets and TPA Ligands. *Org. Lett.*, **2017**, *19*, 4932−4935. DOI: 10.1021/acs.orglett.7b02391

[130] Pavlović, R.Z.; Border, S.E.; Finnegan, T.J.; Zhiquan, L.; Gunther, M.J.; Mū noz, E.; Moore, C.E.; Hadad, C.M.; Badjić, J.D. Twist−turn−twist motif chaperoned inside molecular baskets. *J. Am. Chem. Soc.*, **2019**, *141*, 16600−16604. DOI: 10.1021/jacs.9b09003

[131] Ruan, Y.; Chen, S.; Brown, J.D.; Hadad, C.M.; Badjić, J.D. Ubiquitous assembly of amphiphilic baskets into unilamellar vesicles and their recognition characteristics. *Org. Lett.*, **2015**, *17*, 852−855. DOI: 10.1021/ol503675d

[132] Border, S.E.; Pavlović, R.Z.; Zhiquan, L.; Gunther, M.J.; Wang, H.; Cui, H.; Badjić, J.D. Light-triggered transformation of molecular baskets into organic nanoparticles. *Chem. Eur. J.*, **2019**, *25*, 273–279. DOI: 10.1002/chem.201803693

[133] Border, S.E.; Pavlović, R.Z.; Zhiquan, L.; Gunther, M.J.; Wang, H.; Cui, H.; Badjić, J.D. Photo-induced formation of organic nanoparticles possessing enhanced affinities for complexing nerve agent mimics. *Chem. Commun.*, **2019**, *55*, 1987–1990. DOI: 10.1039/c8cc08938h

[134] Pavlović, R.Z.; Border, S.E.; Li, Y.; Xiaopeng Li, X.; Badjić, J.D. Photoinduced interruption of interannular cooperativity for delivery of cationic guests in water. *Chem. Commun.*, **2020**, *56*, 2987–2990. DOI: 10.1039/c9cc09903d

[135] Zhiquan, L.; Xie, H.; Border, S.E.; Gallucci, J.; Pavlović, R.Z.; Badjić, J.D. A stimuli-responsive molecular capsule with switchable dynamics, chirality, and encapsulation characteristics. *J. Am. Chem. Soc.*, **2018**, *140*, 11091−11100 DOI: 10.1021/jacs.8b06190

[136] Hu, L.; Polen, S.; Hardin, A.M.; Pratumyot, Y.; Hadad, C.M.; Badjić, J.D. On the transfer of chirality, thermodynamic stability, and folding characteristics of stereoisomeric gated baskets. *Eur. J. Org. Chem.*, **2015**, 6832–6840. DOI: 10.1002/ejoc.201501071

[137] Hermann, K.; Pratumyot, Y.; Polen, S.; Hardin, A.M.; Dalkilic, E.; Dastan, A.; Badjić, J.D. Twisted baskets. *Chem. Eur. J.*, **2015**, *21*, 3550–3555. DOI: 10.1002/chem.201406492

[138] Pratumyot, Y.; Chen, S.; Hu, L.; Polen, S.M.; Hadad, C.M.; Badjić, J.D. Assembly and folding of twisted baskets in organic solvents. *Org. Lett.*, **2016**, *18*, 4238−4241. DOI: 10.1021/acs.orglett.6b01976

[139] Pavlović, R.Z.; Zhiquan, L.; Güney, M.; Lalisse, R.F.; Hopf, R.G.; Gallucci, J.; Moore, C.; Xie, H.; Hadad, C.M.; Badjić, J.D. Multivalent C−H···Cl/Br−C interactions directing the resolution of dynamic and twisted capsules. *Chem. Eur. J.*, **2019**, *25*, 13124–13130. DOI: 10.1002/chem.201903006

[140] Chen, S.; Yamasaki, M.; Polen, S.; Gallucci, J.; Hadad, C.M.; Badjić, J.D. Dual-cavity basket promotes encapsulation in water in an allosteric fashion. *J. Am. Chem. Soc.*, **2015**, *137*, 12276−12281. DOI: 10.1021/jacs.5b06041

[141] Chen, S.; Wang, L.; Polen, S.M.; Badjić, J.D. Gating the trafficking of molecules across vesicular membrane composed of dual-cavity baskets. *Chem. Mater.*, **2016**, *28*, 8128−8131. DOI: 10.1021/acs.chemmater.6b04550

[142] Chen, S.; Polen, S.M.; Wang, L.; Yamasaki, M.; Hadad, C.M.; Badjić, J.D. Two-dimensional supramolecular polymers embodying large unilamellar vesicles in water. *J. Am. Chem. Soc.*, **2016**, *138*, 11312−11317. DOI: 10.1021/jacs.6b06562

[143] Wang, L.; Neal, T.; Chen, S.; Badjić, J.D. Multivalent and photoresponsive assembly of dual-cavity baskets in water. *Chem. Eur. J.*, **2017**, *23*, 8829–8833. DOI : 10.1002/chem.201701996

[144] Neal, T.A.; Wang, W.; Zhiquan, L.; Peng, R.; Soni, P.; Xie, H.; Badjić, J.D. A hexavalent basket for bottom-up construction of functional soft materials and polyvalent drugs through a "click" reaction. *Chem. Eur. J.*, **2019**, *25*, 1242–1248. DOI: 10.1002/chem.201805246

[145] Wang, W.; Wang, H.; Zhiquan, L.; Xie, H.; Cui, H.; Badjić, J.D. On the encapsulation and assembly of anticancer drugs in a cooperative fashion. *Chem. Sci.*, **2019**, *10*, 5678–5685. DOI: 10.1039/c9sc01380f

[146] Wang, W.; Finnegan, T.J.; Zhiquan, L.; Zhu, X.; Moore, C.E.; Shi, K.; Badjić, J.D. Tuning the allosteric sequestration of anticancer drugs for developing cooperative nano-antidotes. *Chem. Commun.*, **2020**, *56*, 1271–1274 DOI: 10.1039/c9cc09373g

[147] Sartyoungkul, S.; Yakiyama, Y.; Sakurai, H. Synthesis and dimerization properties of cup- and bowl-shaped cyclic trilactams. *Asian J. Org. Chem.*, **2020**, *9*, 947–952. DOI: 10.1002/ajoc.202000140

[148] Sartyoungkul, S.; Thaveesangsakulthai, I.; Cabello, M.K.E.; Kulsing, C.; Sakurai, H. Application of cup-shaped trilactams for selective extraction of volatile compounds by gas chromatography-mass spectrometry. *Analyst*, **2020**, *145*, 6668–6676. DOI: 10.1039/d0an01061h

[149] Fabris, F.; De Lucchi, O.; Nardini, I.; Crisma, M.; Mazzanti, A.; Mason, S.A.; Lemée-Cailleau, M.–H.; Scaramuzzo, F.A.; Zonta, C. (+)-*syn*-Benzotriborneol an enantiopure C_3-symmetric receptor for water. *Org. Biomol. Chem.*, **2012**, *10*, 2464–2469. DOI: 10.1039/c2ob06774a

[150] Fabris, F.; Pellizzaro, L.; Zonta, C.; De Lucchi, O. A Novel C_3-symmetric triol as chiral receptor for ammonium ions. *Eur. J. Org. Chem.*, **2007**, 283–291. DOI: 10.1002/ejoc.200600673

[151] Longhi, G.; Fabris, F.; Zonta, C.; Fornili, S.L. Molecular dynamics simulation of small water-binding cavitands. *Chem. Phys. Lett.*, **2006**, *423*, 312–316. DOI: 10.1016/j.cplett.2006.03.093

[152] Scarso, A.; Pellizzaro, L.; De Lucchi, O.; Linden, A.; Fabris, F. Gas hosting in enantiopure self-assembled oximes. *Angew. Chem. Int. Ed.*, **2007**, *46*, 4972–4975. DOI: 10.1002/anie.200701123

[153] Tartaggia, S.; Scarso, A.; Padovan, P.; De Lucchi, O.; Fabris, F. Gases as guests in benzocyclotrimer cage hosts. *Org. Lett*., **2009**, *11*, 3926-3929. DOI: 10.1021/ol901621b

[154] Xie, H.; Zhiquan, L.; Pavlović, R.Z.; Gallucci, J.; Badjić, J.D. Stackable molecular chairs. *Chem. Commun.*, **2019**, *55*, 5479–5482. DOI: 10.1039/c9cc01664c

[155] Klärner, F.–G.; Schrader, T. Aromatic interactions by molecular tweezers and clips in chemical and biological systems. *Acc. Chem. Res.*, **2013**, *46*, 967–978. DOI: 10.1021/ar300061c

[156] Yanney, M.; Fronczek, F.R.; Sygula, A. A 2:1 receptor/C_{60} complex as a nanosized universal joint. *Angew. Chem. Int. Ed.*, **2015**, *54*, 11153 –11156. DOI: 10.1002/anie.201505327

[157] Upul, K.G.; Kumarasinghe, R.; Fronczek, F.R.; Valle, H.U.; Sygula, A. Bis-corannulenoanthracene: an angularly fused pentacene as a precursor for barrelene-tethered receptors for fullerenes. *Org. Lett.*, **2016**, *18*, 3054−3057. DOI: 10.1021/acs.orglett.6b01049

[158] Bier, D.; Rose, R.; Bravo-Rodriguez, K.; Bartel, M.; Ramirez-Anguita, J.M.; Dutt, S.; Wilch, C.; Klärner, F.–G.; Sanchez-Garcia, E.; Schrader, T.; Ottmann, C. Molecular tweezers modulate 14-3-3 protein–protein interactions. *Nat. Chem.*, **2013**, *5*, 234-239. DOI: 10.1038/NCHEM.1570

[159] Weil, T.; Groß, R.; Röcker, A.; Bravo-Rodriguez, K.; Heid, C.; Sowislok, A.; Le, M.–H.; Erwin, N.; Dwivedi, M.; Bart, S.M.; Bates, P.; Wettstein, L.; Müller, J.A.; Harms, M.; Sparrer, K.; Ruiz-Blanco, Y.B.; Stürzel, C.M.; von Einem, J.; Lippold, S.; Read, C.; Walther, P.; Hebel, M.; Kreppel, F.; Klärner, F.–G.; Bitan, G.; Ehrmann, M.; Weil, T.; Winter, R.; Schrader, T.; Shorter, J.; Sanchez-Garcia, E.; Münch, J. Supramolecular mechanism of viral envelope disruption by molecular tweezers. *J. Am. Chem. Soc.*, **2020**, *142*, 17024−17038. DOI: 10.1021/jacs.0c06400